AWARD NUMBER: W81XWH-18-1-0016

TITLE: Targeted Inhibition of Leukemia Inhibitory Factor (LIF)/LIFR Axis for the Treatment of Triple-Negative Breast Cancer

PRINCIPAL INVESTIGATOR: Dr. RATNA VADLAMUDI

CONTRACTING ORGANIZATION: University of Texas Health Science Center at San Antonio

REPORT DATE: FEBRUARY 2021

TYPE OF REPORT: Annual Report

PREPARED FOR: U.S. Army Medical Research and Materiel Command
Fort Detrick, Maryland 21702-5012

REPORT DOCUMENTATION PAGE

Form Approved
OMB No. 0704-0188

1. REPORT DATE	2. REPORT TYPE	3. DATES COVERED
FEBRUARY 2021	Annual Report	02/01/2020 – 1/31/2021

4. TITLE AND SUBTITLE
Targeted Inhibition of Leukemia Inhibitory Factor (LIF)/LIFR Axis for the Treatment of Triple-Negative Breast Cancer

5a. CONTRACT NUMBER
W81XWH-18-1-0016

5b. GRANT NUMBER
BC170312P1

5c. PROGRAM ELEMENT NUMBER

6. AUTHOR(S)

RATNA VADLAMUDI and BINDU SANTHAMMA

E-Mail: vadlamudi@uthscsa.edu;

5d. PROJECT NUMBER

5e. TASK NUMBER

5f. WORK UNIT NUMBER

7. PERFORMING ORGANIZATION NAME(S) AND ADDRESS(ES)
University of Texas Health Science Center at San Antonio

7703 Floyd Curl Drive
San Antonio, Texas 78229

8. PERFORMING ORGANIZATION REPORT NUMBER

9. SPONSORING / MONITORING AGENCY NAME(S) AND ADDRESS(ES)

U.S. Army Medical Research and Materiel Command
Fort Detrick, Maryland 21702-5012

10. SPONSOR/MONITOR'S ACRONYM(S)

11. SPONSOR/MONITOR'S REPORT NUMBER(S)

12. DISTRIBUTION / AVAILABILITY STATEMENT

Approved for Public Release; Distribution Unlimited

13. SUPPLEMENTARY NOTES

14. ABSTRACT

Leukemia inhibitory factor receptor (LIFR) and its ligand LIF play a critical role in cancer progression and therapy resistance. In this DOD funded project, we developed a first-in-class inhibitor of LIFR, EC359, which binds to LIFR and block LIF/LIFR interactions. EC359 treatment exhibited antiproliferative effects, reduces invasiveness and stemness, and promoted apoptosis in triple-negative breast cancer (TNBC) cell lines. Treatment with EC359 attenuated the activation of LIF/LIFR-driven pathways. EC359 also reduced the viability of therapy resistant TNBC models and enhanced HDAC inhibitors therapy. Further, EC359 significantly reduced tumor progression in TNBC xenografts, and patient-derived xenografts (PDX). EC359 exhibits distinct pharmacologic advantages, including oral bioavailability, and *in vivo* stability. Collectively, these data support EC359 as a novel targeted therapeutic that inhibits LIFR oncogenic signaling.

15. SUBJECT TERMS
Breast cancer; TNBC, LIFR, LIF, STAT3, tumor progression

16. SECURITY CLASSIFICATION OF:			17. LIMITATION OF ABSTRACT	18. NUMBER OF PAGES	19a. NAME OF RESPONSIBLE PERSON USAMRMC
a. REPORT	b. ABSTRACT	c. THIS PAGE			19b. TELEPHONE NUMBER *(include area code)*
Unclassified	Unclassified	Unclassified	Unclassified	37	

Table of Contents

1. INTRODUCTION

Triple negative breast cancer (TNBC) has poor prognosis, lack targeted therapies, contain high percentage of cancer stem cells, and often exhibit therapy resistance. TNBC are more aggressive, and due to lack of targeted therapies, they represent a disproportional share of the breast cancer mortality. TNBC tumors are characterized by high propensity to metastasis, some subtypes of TNBC such as claudin-low are highly enriched with cancer stem cells and frequently exhibit therapy resistance. The propensity of TNBC to metastasize to visceral sites is another major clinical problem and identifying factors that contribute to metastases are needed for advancement of therapies. There is a major need for rationally designed novel therapies that can improve response to TNBC treatment and extend survival.

Leukemia inhibitory factor (LIF) is the most pleiotropic member of the interleukin-6 family of cytokines that signals via the LIF receptor (LIFR). LIF activate multiple signaling pathways including STAT3, MAPK, AKT, and mTOR that are implicated in TNBC progression. Recent evidence implicated tumors exhibit upregulated LIF-LIFR signaling via autocrine and paracrine mechanisms. LIF promotes proliferation and metastasis of breast cancer cells. TNBC cells have higher expression of LIF compared to ER-positive breast cancer cells and overexpression of LIF significantly associated with a poorer relapse free survival in breast cancer patients. LIF signaling play a role in crosstalk between tumor cells and fibroblasts and mediate pro-invasive activation of stromal fibroblasts. LIF-LIFR axis is implicated in the maintenance of stem cells and deregulation of LIF signaling contribute to chemoresistance. Together, these emerging findings strongly suggest that LIF signaling in TNBC may be clinically actionable and that disruption of the LIF signaling has potential to block TNBC progression.

With our expertise in developing novel small molecule inhibitors that disrupt protein-protein interactions and SAR studies using our compound libraries, we have rationally designed and synthesized a first-in class LIF inhibitor compound. The objective of this proposal is to confirm the specificity, test in vivo activity and establish the mechanism, and conduct safety, efficacy, off target screening studies. Our hypothesis is that LIFR signaling play a critical role in TNBC progression and disruption of LIF-LIFR interaction with small molecule inhibitor EC359 will have therapeutic effect.

2. KEYWORDS

Breast cancer; TNBC; LIFR; LIF; STAT3; xenograft; tumor progression;

3. ACCOMPLISHMENTS

During the past 12 months of the project, from February 1, 2020 to January 31, 2021, we have made significant progress in completing the proposed experiments as detailed in section 3.2. Because of COVID few animal experiments were delayed. However, they are on schedule to be completed during the no cost extension period. Major accomplishments include completion of EC359 signaling experiments, completions of invasion studies, completion of studies testing the utility of EC359 in treating therapy resistance, completion of second xenograft and two additional PDX models studies, completion of large scale synthesis of EC359, completion of toxicity and PK studies. **All the results obtained during third year were shown in blue color font** and year 1 and year 2 results are shown in black color font. In addition, we have presented the results from third year as an abstract in 2020 AACR and a new manuscript was submitted to nature communications biology.

3-1. What were the major goals of the project?

Aim 1. To establish the efficacy of EC359 using preclinical, syngeneic and PDX models of TNBC.

Aim 2. To establish the molecular mechanism of action of EC359 and to identify potential biomarkers.

Aim 3. To establish ADME, pharmacokinetics (PK), and toxicology of EC359.

3-2. What was accomplished under these goals?

Major task 1: To establish the efficacy of EC359 using preclinical, syngeneic and PDX models of TNBC.

Subtask 1: To characterize the biological activity of EC359 in vitro (Time line 1-12 months)

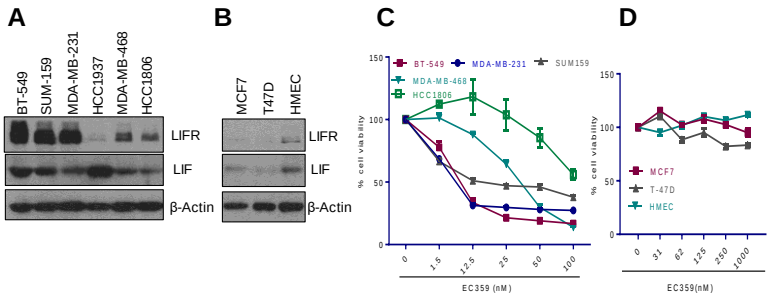

Fig 1. The expression of LIF and LIFR in TNBC (**A**), ER+ve breast cancer and normal mammary epithelial cells (**B)** was determined by western blotting. Effect of increasing doses of EC359 on the cell viability of TNBC (**C**) ER+ breast cancer and normal mammary epithelial cells (**D**) was determined using the MTT cell viability assay (n=3).

<u>EC359 reduced the cell viability of LIF and LIFR expressing cells.</u> We first examined the expression of LIF and LIFR in cells that represent various subtypes of TNBC (BT-549, SUM-159, MDA-MB-231, HCC1937, MDA-MB-468, and HCC1806), ER+ve breast cancer (MCF7, and T47D) as well as normal mammary epithelial cells (HMEC). We found that five of the six TNBC cells expressed high levels of LIF and LIFR when compared to ER+ve breast cancer cells and normal cells (Figure 1A,B). Next, we examined the efficacy of EC359 on cell viability of TNBC and ER+ve breast cancer cells. Treatment with EC359 resulted in a significant dose-dependent reduction in the cell viability of TNBC cells (IC50 10-50 nM) and their inhibition is correlated well with the LIF and LIFR expression levels (Figure 1C). Interestingly ER+ve breast cancer cells which express low levels of LIF and LIFR exhibited low sensitivity to EC359 treatment (IC50 >1000 nM) when compared with TNBC cells (Figure 1D).

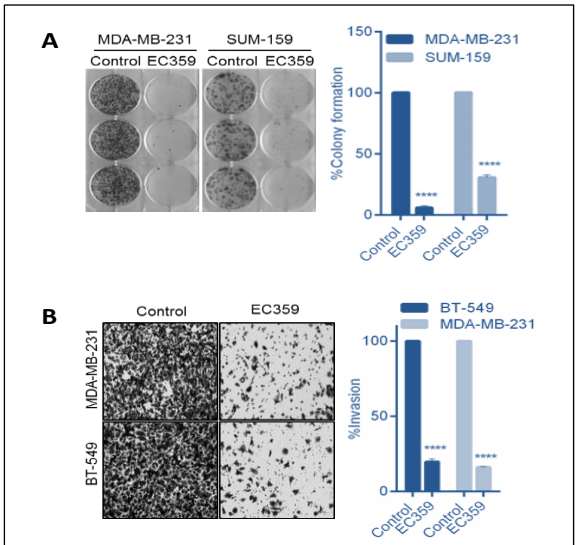

Figure 2.**A**, Effect of EC359 (20nM) on cell survival was measured using colony formation assays. **B**, Effect of EC359 on cell invasion of MDA-MB-231 and BT-549 model cells was determined using matrigel invasion chamber assays (n=3) (EC359 25nM). Representative images of invaded cells are shown and the number of invaded cells in five random fields was quantitated. * P<0.05, ** P<0.01, *** P<0.001, ****p<0.0001.

<u>EC359 reduced survival and invasion of TNBC cells</u>. We next examined the efficacy of the EC359 on the survival of TNBC cells. In clonogenic survival assays, EC359 significantly reduced the colony formation ability of MDA-MB-231 and SUM-159 cells (Figure 2A). Given the important role of the LIF axis in the invasiveness of cancer cells, we examined the effect of EC359 in reducing the invasion of TNBC cells. Matrigel invasion assays demonstrated that EC359 significantly reduced the invasion potential of MDA-MB-231 and BT-549 cells (Figure 2B). Collectively, these results suggest that EC359 exhibits significant inhibitory activity on invasion of TNBC cells.

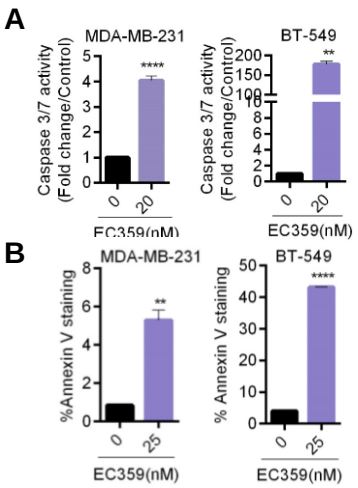

Figure 3. **A**, Effect of indicated doses of EC359 on caspase 3/7 activity (Caspase-Glo3/7 assay) and I, Annexin V staining in MDA-MB-231 and BT-549 cells (n=3) was determined. ** P<0.01, ****p<0.0001

<u>EC359 induced apoptosis of TNBC cells (Year 2 studies)</u>

We examined whether EC359 induce apoptosis of TNBC cells using caspase 3/7 activity assay and Annexin V staining assay. EC359 treatment significantly increased caspase 3/7 activity (Figure 3A) and Annexin V positive cells (Figure 3B) in both MDA-MB-231 and BT-549 cells. Collectively, these results suggest that EC359 promotes apoptosis of TNBC cells.

Multi-PI contributions: The above work was jointly performed by Dr. Vadlamudi and Dr. Santhamma labs. Dr. Santhamma lab generated needed EC359, and tested its purity and activity. Dr. Vadlamudi lab characterized biological activity using TNBC models.

Subtask 2: Test the efficacy of EC359 on blocking TNBC tumorigenesis in vivo (Time line 6-24 months)

IACUC and ACURO Approval: Approvals have been obtained and these experiments were ongoing

EC359 reduced TNBC xenograft tumor growth in vivo: To test the efficacy of EC359 on *in vivo* tumor progression, we established MDA-MB-231 xenograft tumors in the mammary fat pad of nude mice. Mice were randomized to vehicle (hydroxy methyl cellulose) and EC359 (5 mg/kg/day via subcutaneous injection) 3 days/week. EC359 treatment significantly reduced the tumor progression compared to vehicle (Figure 4A). Mice body weights in the vehicle and EC359 treated groups were similar (Figure 4B) confirming the low toxicity of EC359. Further, EC359 treated tumors exhibited fewer proliferating cells (Ki-67 positive cells) compared to vehicle treated tumors (Figure 4C). Further, RTqPCR analysis confirmed significant decrease in the activation of STAT3 target genes in EC359 treated tumors compared to control (Figure 4D). Western blot analysis confirmed that xenograft tumors express LIFR and LIF (Figure 4E). Further, EC359 treatment substantially reduced the phosphorylation of STAT3 and ERK1/2 pathways in EC359 treated tumors compared to vehicle treated tumors (Figure 3E).

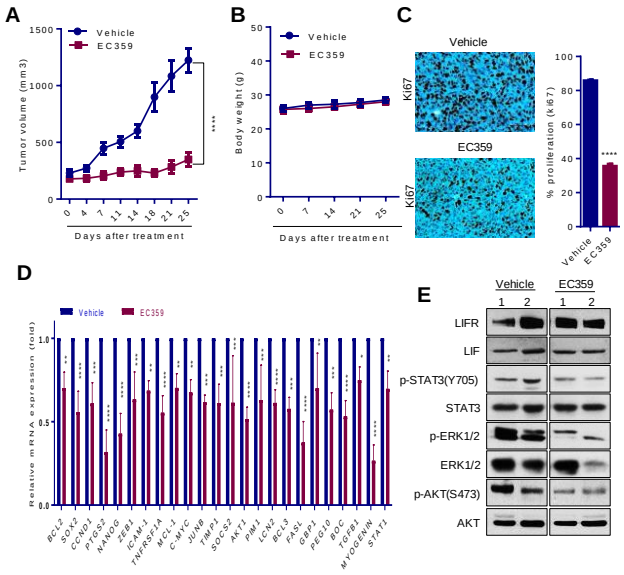

Figure 4. **A**, MDA-MB-231 xenografts (n=7) were treated with vehicle or EC359 (5mg/kg/s.c./3 days/week). Tumor volumes are shown in the graph. **B**, Body weights of vehicle and EC359 treated mice are shown. **C**, Ki-67 expression as a marker of proliferation was analyzed by IHC and quantitated. **D**, Status of STAT3 target genes were measured by using RT-qPCR analysis (n=3). **E**, LIFR downstream signaling was measured using western blotting (data using two different xenograft tumors is shown). * P<0.05, ** P<0.01, *** P<0.001, ****p<0.0001.

We have also tested the utility of EC359 using a second TNBC xenograft model (MDA-MB-468). MDA-MB-468 xenografts bearing SCID mice were randomized and treated with vehicle or EC359 (5mg/kg/sc) 3 days/week. EC359 treatment resulted in significantly lower tumor volume compared to vehicle (Fig. 5a). IHC analyses revealed that MDA-MB-468 xenografts treated with EC359 showed decreased proliferation as measured by Ki67 compared to control (Fig. 5b,c). Collectively, these results suggest that EC359 has potent anti-tumor activity on TNBC in preclinical models.

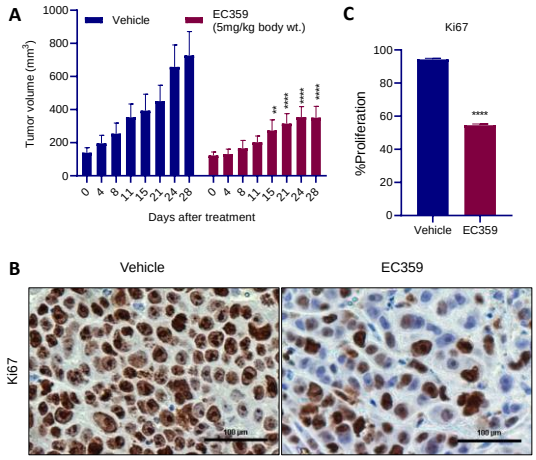

Figure 5. A. MDA-MB-468 (n=8) xenografts in SCID mice were treated with vehicle or EC359 (5 mg/kg/day). Tumor volume (**A**) and proliferation (KI staining) was measured. Error bars represent SEM (**B,C**).

Multi-PI contributions: The above work was jointly performed by Dr. Vadlamudi and Dr. Santhamma labs. Dr. Santhamma lab synthesized needed EC359 compound and optimized process development. Dr. Vadlamudi's lab conducted xenograft studies, tumor measurement and biochemical characterization.

Subtask 3: Effect of EC359 on blocking TNBC tumor progression to metastasis (Time line 12-36 months)

During third year, we examined the potential of EC359 in reducing invasion of TNBC cells. Matrigel invasion assays demonstrated that combination therapy of EC359+HDACi is more effective in reducing the invasion of MDA-MB-231 and BT-549 cells (Fig. 2c, d). We will examine the effect of EC359 in blocking the tumor progression using xenograft models during the no cost extension period.

Subtask 4: Test the efficacy of EC359 combination therapy in reducing the growth of therapy resistant TNBC in vivo (Time line 24-36 months).

In vitro MTT assays demonstrated synergistic activity of EC359 with chemotherapeutic agents, cisplatin, and paclitaxel (Fig. 7, top panel). Further, EC359 is also effective in reducing the cell viability of paclitaxel resistant TNBC model cells (Fig. 7, bottom panel).

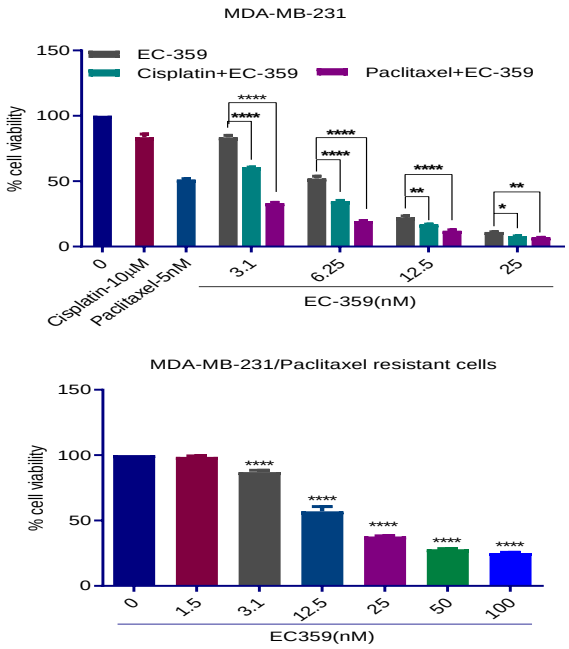

Figure 7: MDA-MB 231 cells or paclitaxel resistant MDA-MB-231 cells were treated with EC359 alone or in combination with cisplatin or paclitaxel and cell viability was measured using MTT assay. **** P<0.0001.

Recent studies suggested that HDACi treatment promotes expression and activation of LIFR, which restrains the efficacy of HDACi as TNBC therapeutics. We examined whether treatment of EC359 enhances the therapeutic efficacy of HDACi on TNBC cells using MTT assays. As shown in Fig. 8, addition of EC359 significantly enhanced the efficacy of HDACi in reducing cell viability compared to HDACi as monotherapy. Results showed that the combination index (CI) values were less than 1 in all the three HDACi combinations tested and confirmed that the combination therapy was synergistic (Fig. 8A). In clonogenic survival assays, EC359 enhanced HDACi ability to reduce the colony formation of MDA-MB-231 and BT-549 cells (Fig. 8B) compared to monotherapy.

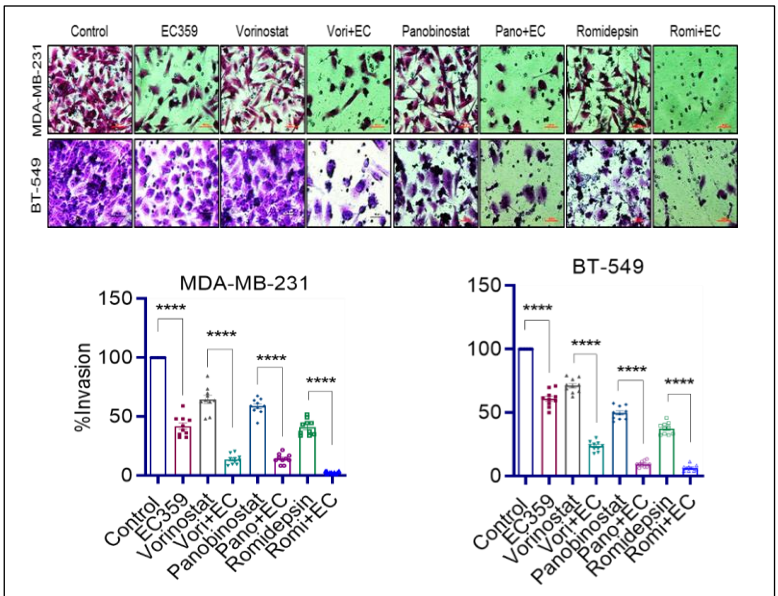

Figure 6. Effect of EC359+HDACi combination therapy on cell invasion of MDA-MB-231 and BT-549 model cells was determined using Matrigel invasion chamber assays. Data are representative of three independent experiments (n=3). Representative images of invaded cells are shown and the number of invaded cells in five random fields were quantitated. **** P<0.0001

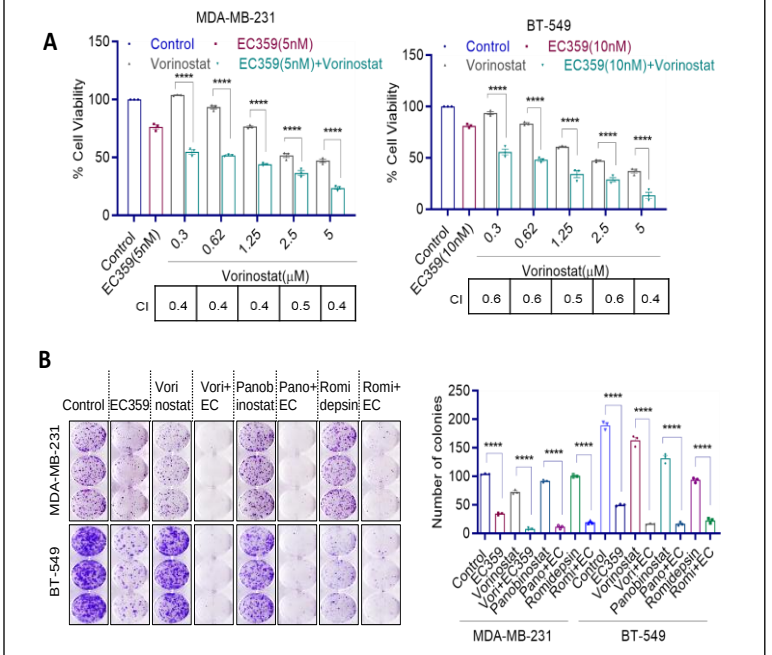

Figure 8. MDA-MB-231 and BT-549 cells were treated with indicated concentrations of vorinostat (**A**), for 72 h in the presence or absence of EC359 (MDA-MB-231:5 nM; BT-549:10 nM) and the cell viability was measured by MTT assay. **B**, Effect of EC359+HDACi combination therapy on the cell survival of TNBC cells measured using colony formation assays (n=3). Representative images from three independent experiments are shown, and quantitation of colonies is presented next to the images. **** P<0.0001.

Subtask 5: Test the efficacy of EC359 in reducing the growth of TNBC PDX tumors in vivo (Time line 18-36 months)

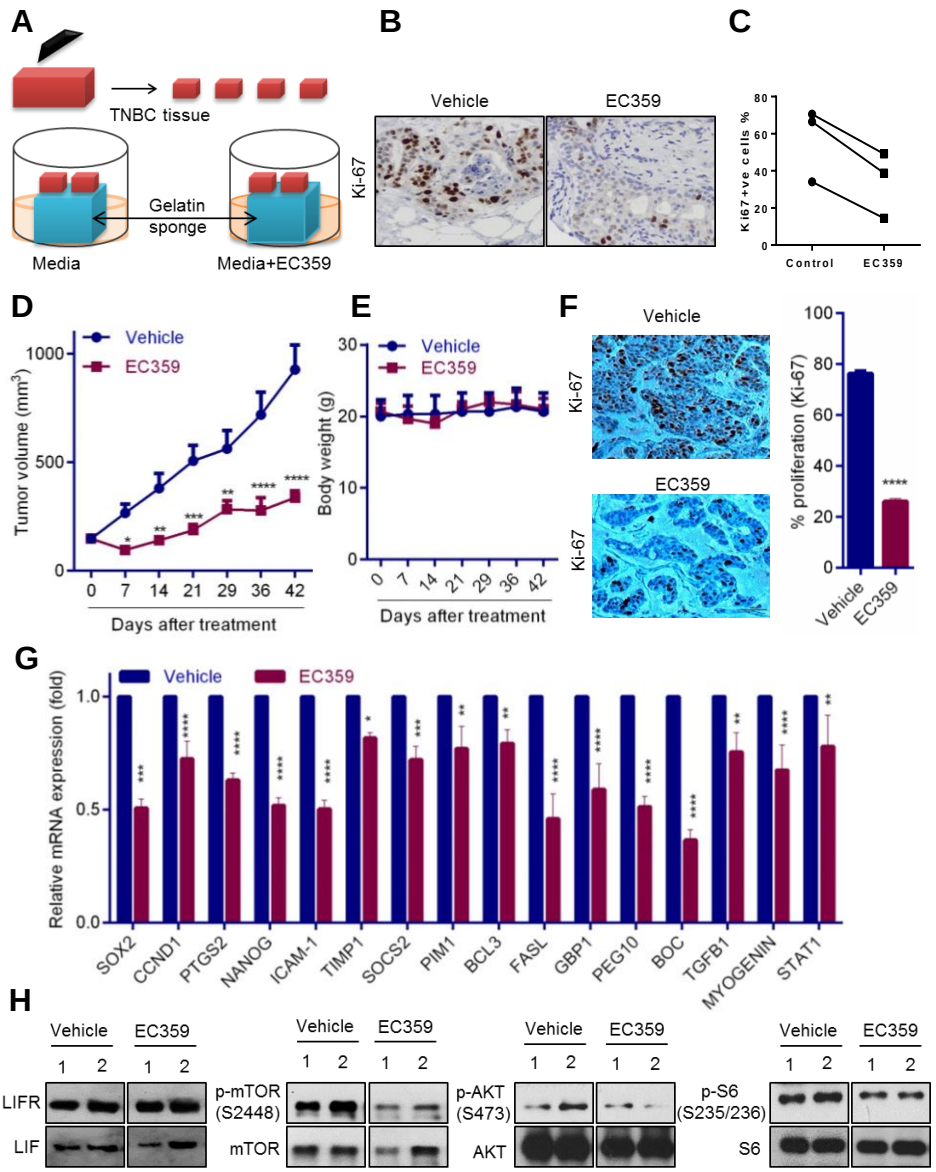

Figure 9. EC359 decreases the growth of patient-derived explants (PDEx) *ex vivo* and PDX tumors *in vivo.* **A**, Schematic representation of *ex vivo* culture model. **B**, TNBC explants were treated with EC359 for 72 h and the proliferation was determined using Ki-67 immunostaining. Representative Ki-67 staining from one tumor treated with vehicle or EC359 is shown. **C**, The Ki67 expression in TNBC explants (n=3) is quantitated. **D**, TNBC PDX tumors (n=6) were treated with vehicle or EC359 (10mg/kg/s.c./3 days/week). Tumor volumes are shown in the graph. **E**, Body weights of vehicle and EC359 treated mice are shown. **F**, Ki-67 expression as a marker of proliferation was analyzed by IHC and quantitated. **G**, STAT3 target genes were measured by using RT-qPCR analysis (n=3). **H**, Status of LIFR downstream signaling was measured using western blotting (data using two different PDX tumors is shown). * P<0.05, ** P<0.01, *** P<0.001, ****p<0.0001.

<u>EC359 has activity against primary patient derived TNBC explants and reduced in vivo tumor progression in PDX model</u> (Year 2 studies). We tested the utility of EC359 using an *ex vivo* culture model of primary breast tumors, which allowed for the evaluation of drugs on human tumors while maintaining their native tissue architecture (Figure 5A). Briefly, surgically extirpated de-identified TNBC tumor tissues were cut into small pieces and placed on gelatin sponge soaked in the culture medium and grown for a short term in the presence of vehicle or EC359 (Figure 5A). Treatment of TNBC explants with EC359 substantially decreased their proliferation (Ki-67 positivity) compared to vehicle treated tumors (Figure 9 B,C). Next, we tested the effect of EC359 on PDX tumor growth in vivo. EC359 treatment significantly reduced the tumor progression compared to the vehicle treated control group (Figure 9D) and did not affected body weight (Figure 9E). EC359 treated PDX tumors exhibited fewer proliferating cells compared to vehicle treated tumors (Figure 5F). RT-qPCR analysis confirmed a significant decrease in the activation of STAT3 target genes in EC359 treated mice (Figure 9G). Western blot analysis confirmed that PDX tumors express LIFR and LIF (Figure 5H). Furthermore, EC359 treatment substantially reduced the phosphorylation of mTOR, S6 and AKT in tumors compared to vehicle treated tumors (Figure 9H). We validated these results using two additional PDX models (Fig. 10). Results showed that EC359 is efficient in reducing the PDX tumor growth compared to vehicle (Fig. 10 A,B). Further, EC359 treated tumors showed less proliferation (Ki67 staining) compared to vehicle (Fig. 10 A,B). These results suggest that EC359 has therapeutic

activity on primary patient derived TNBC explants and PDX tumors.

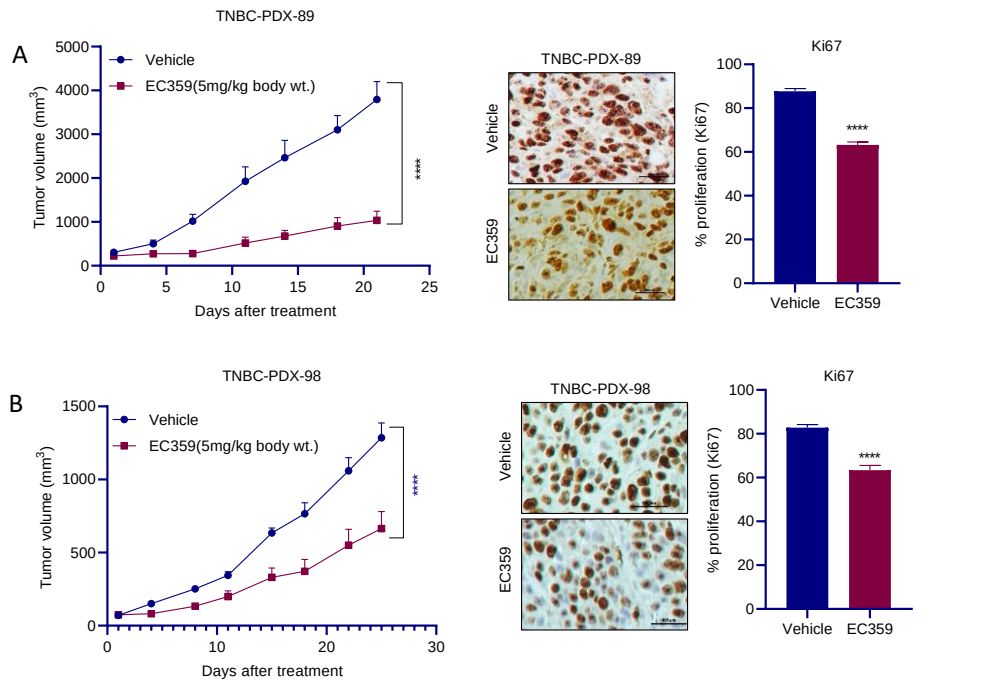

Figure 10. Female SCID mice were implanted with 2 mm^3 pieces of PDX tumors TM00089 (**a**), TM00098 (**b**) into the flanks and randomized for treatment when the tumor volume reached ~150 mm^3. TNBC PDX tumors (n=6-8) were treated with vehicle or EC359. Tumor volumes are shown in the graph. Ki67 expression as a marker of proliferation was analyzed by IHC and quantitated.

Major Task 2: To establish the molecular mechanism of action of EC359 and to identify potential biomarkers

Subtask 1: Determine the specificity of EC359 for targeting LIFR (Time line 1-12 months)

Surface plasmon resonance (SPR) studies confirmed EC359 direct interaction with LIFR. To test whether EC359 directly binding to LIFR complex, binding profiles of EC359 to LIF/LIFR were evaluated using surface plasmon resonance (SPR). Two sets of studies were performed: 1) to verify the integrity of recombinant proteins, the interaction between LIFR and LIF was studied; 2) small molecule binding to LIF/LIFR by either immobilizing LIFR or LIF onto a sensor chip was tested. Results from the first set of studies confirmed the integrity of recombinant LIF and LIFR; LIF bound to immobilized LIFR-Fc with a binding constant of 7µM (Figure 11A). In the second set of studies, results showed EC359 binding to LIFR, but not LIF. Further, EC359 bound to LIFR in a dose dependent manner with KD 81µM (Figure 11B). The results confirmed that EC359 is a specific inhibitor of LIF/LIFR complex.

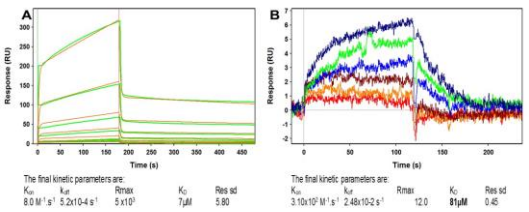

Fig 11. SPR studies. A, Confirmation of functionality of LIF/LIFR interaction. B, Confirmation of LIFR-EC359 interaction

Microscale thermophoresis (MST) assays revealed high affinity interaction of EC359 with LIFR. Since SPR studies use immobilized receptor complex, we conducted an orthogonal assay where receptor is not immobilized to verify EC359 binding to the receptor complex. MST is a powerful technique to quantify biomolecule interactions. By combining the precision of fluorescence detection with the variability and sensitivity of thermophoresis, MST provides a flexible, robust and fast way to dissect molecular interactions. MST analysis confirmed direct interaction of EC359 with LIFR with an estimated KD of 10.2 nM (Figure 12).

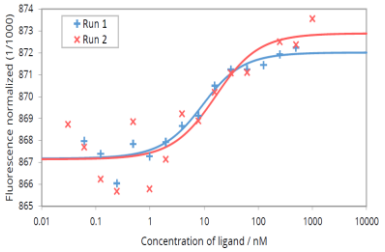

Fig 12. Binding of EC359 to LIFR was confirmed using MST assays.

CRISPR KO cells confirmed requirement of LIFR for EC359 function. To further confirm the target specificity of EC359, we generated doxycycline inducible LIFR-KO cells using Cas9 stably expressing TNBC cells. Results

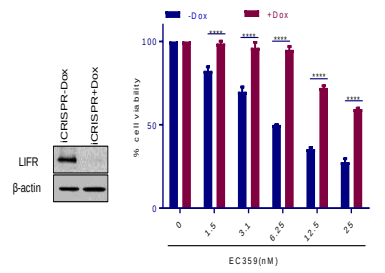

Fig 13. Effect of inducible CRISPR/Cas9 mediated KO of LIFR on EC359 induced cell viability was determined using MTT assays in BT-549 cells (n=3).

indicated a reduction of LIFR expression in BT-549 models contributed to the resistance of the EC359 mediated decrease in cell viability (Figure 13). Collectively, this data suggests that EC359 activity depends on presence of functional LIF/LIFR signaling axis in cells.

Multi-PI contributions: The above work was jointly performed by Dr. Vadlamudi and Dr. Santhamma labs. Dr. Santhamma lab completed biophysical studies charactering EC359 interaction with LIFR including SPR and MST studies. Dr. Vadlamudi's lab generated CRISPR KO cells and completed MTT assays.

Subtask 2: Test the effect of effect of EC359 on LIF-LIFR signaling

EC359 reduced LIFR mediated activation of downstream signaling pathways. To further confirm the effect of EC359 on LIF/LIFR downstream signaling pathways, MDA-MB-231 and BT-549 cells were pretreated with vehicle or EC359 and subsequently stimulated with LIF. STAT3 activation was examined using western blotting. EC359 treatment substantially reduced the LIF activation of STAT3 in both BT-549 and MDA-MB-231 cells (Figure 14A). Further, EC359 treatment also substantially decreased the phosphorylation of AKT, mTOR, S6 and ERK1/2 in MDA-MB-231 and BT-549 cells (Figure14 B,C). EC359 treatment also increased the phosphorylation of proapoptotic p38MAPK in BT-549 cells (Figure 14C). These results suggest that EC359 acts as a LIFR inhibitor and atten uates LIFR mediated signaling in TNBC cells.

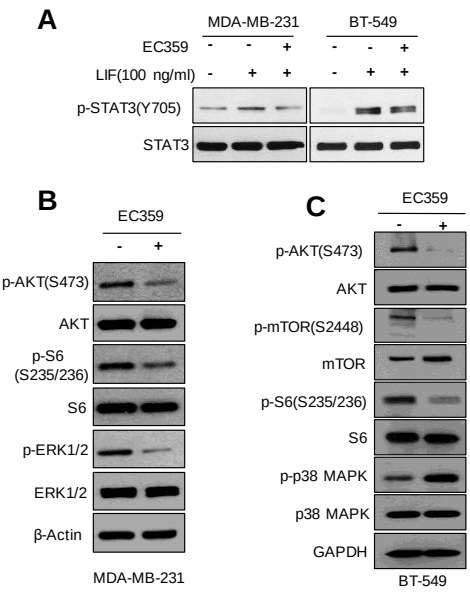

Fig 14. **A**, MDA-MB-231 and BT-549 cells were serum starved for 24 h, pretreated with EC359 (100nM) for 1 h and then stimulated with LIF (10min) and the status of STAT3 phosphorylation was measured using western blotting. **B, C**, MDA-MB-231, BT-549, were treated with EC359 (100 nM) and status of LIFR downstream signaling was measured using western blotting.

EC359 inhibited LIFR mediated transcriptional changes (year 2 studies). LIF/LIFR activates multiple signaling pathways including JAK/STAT3, MAPK, AKT, and mTOR; all of which are implicated in TNBC progression. To confirm the inhibitory effect of EC359 on LIF/LIFR mediated STAT3 activation, BT-549 cells that stably express STAT3-Luc reporter were pretreated with vehicle or EC359 followed by stimulation with LIF. As expected, LIF treatment significantly increased the STAT3 reporter activity and this activation was inhibited by EC359 treatment (Figure 15A). Since our modeling studies predicted EC359 interaction with the ligand binding interface of LIFR, we examined whether EC359 also blocks signaling by other LIFR ligands such as Oncostatin M (OSM), Ciliary Neurotrophic Factor (CNTF), and Cardiotrophin 1 (CTF1). Results showed that EC359 blocked the OSM, CNTF and CTF1 mediated STAT3 activity in BT-549 cells (Figure 10A). We also confirmed that EC359 has the ability to block LIF, OSM, CNTF and CTF1 mediated STAT3 activation using MDA-MB-231 cells stably expressing STAT3-Luc reporter (Figure 15B).

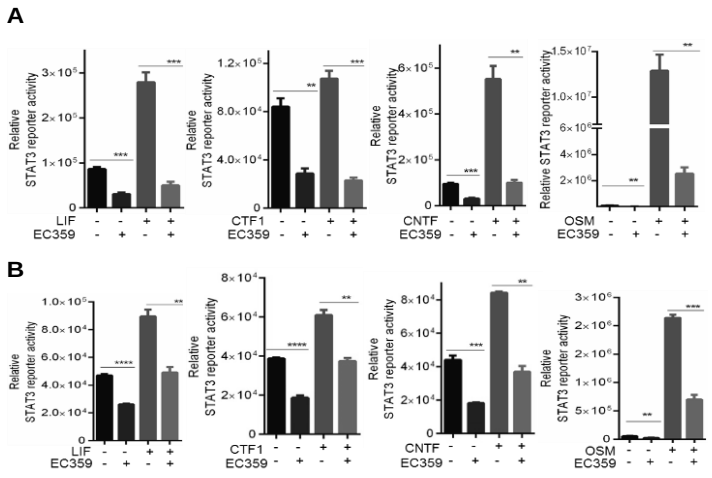

Fig 15. Effect of EC359 on LIFR mediated transcription in TNBC cells. BT-549 (**A**) and MDA-MB-231 (**B**) cells stably expressing STAT3-luc reporter were serum starved for 24 h, pretreated with EC359 (50 nM) for 1 h and then stimulated with indicated concentrations of LIF, CTF1, OSM, CNTF (n=3). Reporter activity was measured after 24 h. **C**, Effect of EC359 (100 nM) treatment (12 h) on STAT3 targeted genes was measured using RT-qPCR analysis (n=3). ** P<0.01, *** P<0.001, ****p<0.0001

Multi-PI contributions: The above work was jointly performed by Dr. Vadlamudi and Dr. Santhamma labs. Dr. Santhamma lab synthesized needed EC359 and optimized process development. Dr. Vadlamudi's lab conducted signaling and western studies. Both labs collectively interpreted the data.

Subtask 3: Test the effect of EC359 on TNBC signaling pathways. (Time line 1-24 months)

Effect of EC359 on TNBC signaling pathways (Year 2 studies). To address pathways/genes modulated by EC359, we analyzed the transcriptional changes following treatment with EC359. MDA-MB-231 cells were treated with vehicle or EC359 treatment for 6 h, and the isolated RNA was utilized for a global transcriptome analysis using RNA-Seq. In particular, 543 genes ($p < 0.05$) were differentially expressed in EC359–treated cells compared to vehicle-treated cells with 268 genes down-regulated and 275 genes upregulated. A representative heat map of differentially expressed genes is shown in Fig. 16a. The biological significance of the differentially expressed genes was determined using Ingenuity Pathway Analysis (IPA). IPA analysis revealed that EC359 treatment significantly modulated the genes involved in several pathways including JAK/STAT3, mTOR and OSM (Fig. 16b). In RT-qPCR assays using BT-549 cells, EC359 treatment significantly reduced the expression of several known STAT3 target genes (Figure 16C).

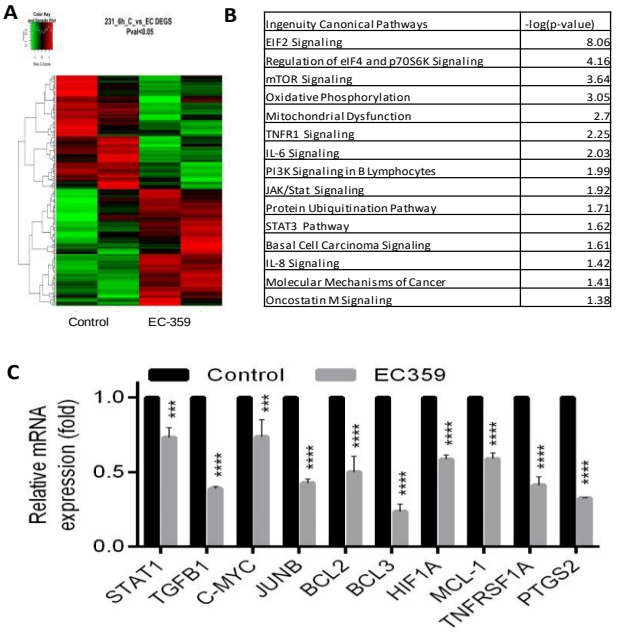

Ingenuity Canonical Pathways	-log(p-value)
EIF2 Signaling	8.06
Regulation of eIF4 and p70S6K Signaling	4.16
mTOR Signaling	3.64
Oxidative Phosphorylation	3.05
Mitochondrial Dysfunction	2.7
TNFR1 Signaling	2.25
IL-6 Signaling	2.03
PI3K Signaling in B Lymphocytes	1.99
JAK/Stat Signaling	1.92
Protein Ubiquitination Pathway	1.71
STAT3 Pathway	1.62
Basal Cell Carcinoma Signaling	1.61
IL-8 Signaling	1.42
Molecular Mechanisms of Cancer	1.41
Oncostatin M Signaling	1.38

Fig 16. A Total RNA was isolated from the MDA-MB-231 cells that were treated with either vehicle or EC359 for 6 h and subjected to RNA sequencing. The heat map of differentially expressed genes between vehicle and EC359 is shown. B, Differentially expressed genes were subjected to pathway analysis using IPA software and the selected top canonical pathways modulated by EC359 are shown. C, Effect of EC359 (100 nM) treatment (12 h) on STAT3 targeted genes was measured using RT-qPCR analysis (n=3). ** P<0.01, *** P<0.001, ****p<0.0001

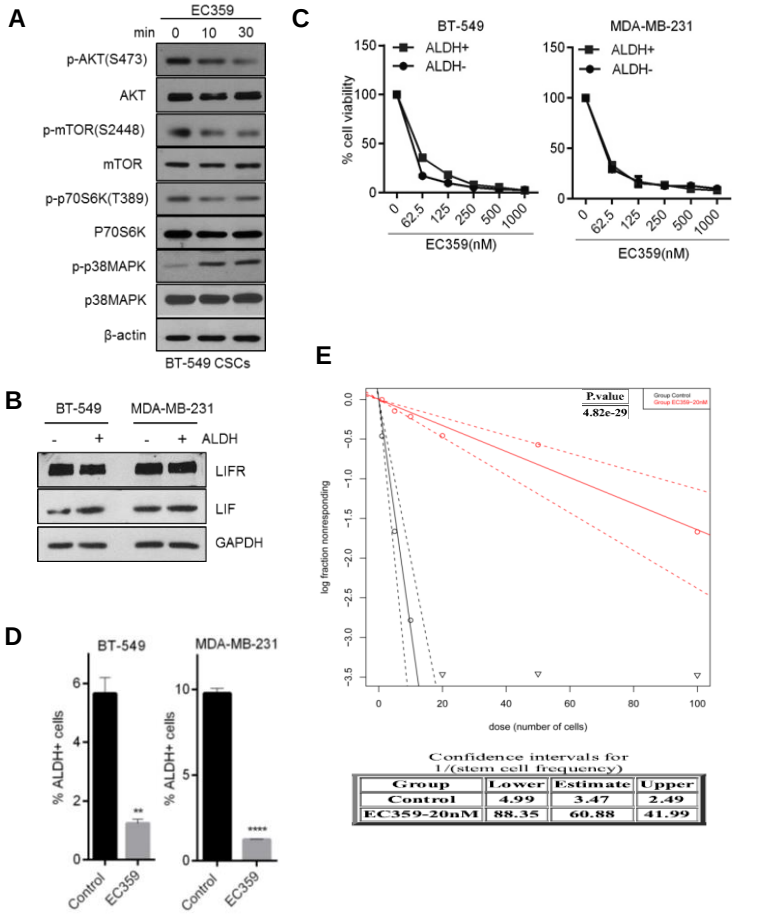

Group	Lower	Estimate	Upper
Control	4.99	3.47	2.49
EC359-20nM	88.35	60.88	41.99

Fig 17. EC359 treatment reduced stemness of TNBC cells. A, CSCs were treated with EC359 (100 nM) and status of LIFR downstream signaling was measured using western blotting. B, ALDH + and ALDH- cells were isolated by FACS and the expression levels of LIFR and LIF were measured by western blotting. C, Effect of EC359 on the viability of ALDH+ (CSCs) and ALDH- (non CSCs) cells was determined using cell titer glo assay (n=3). D, BT-549 and MDA-MB-231 cells were treated with EC359 (100 nM) and the status of ALDH+ cells was determined by FACS analysis. E, Effect of EC359 on self-renewal of cancer stem cells was determined by extreme limiting dilution assays.

Subtask 4: Test the Effect of EC359 on TNBC Stemness (Time line 12-36 months)

EC359 reduced the cell viability and self-renewal of TNBC stem cell. (Year 2 studies). The LIF/LIFR axis plays a vital role in stemness. To test the effect of EC359 on stemness, cancer stem cells (CSCs) were isolated from MDA-MB-231 and BT-549 using ALDH+ flow cytometry sorting. EC359 treatment substantially decreased the phosphorylation of AKT, mTOR, p70S6K, and increased phosphorylation of proapoptotic p38MAPK in CSCs (Figure 17A). Western blot analysis showed that ALDH+ (CSCs) and ALDH- (differentiated) cells have similar levels of LIFR

(Figure 17 B). Further, in cell viability assays, EC359 similarly inhibited both ALDH+ and ALDH- cells (Figure 17 C). Further, pretreatment of TNBC cells with EC359 significantly reduced the abundance of ALDH+ cells (Figure 12D). To further study the effect of EC359 on the self-renewal ability of CSCs, extreme limiting dilution assays (ELDA) were performed. Results showed that EC359 significantly reduced the self renewal of CSCs compared to control (Figure 17E).

Major Task 3: To establish ADME, pharmacokinetics (PK), and toxicology of EC359

Subtask 1: To synthesize EC359 in large quantities.

The specific aim for the chemistry part involved the synthesis of enough quantities of EC359 for preclinical *in vitro* as well as *in vivo* studies. During first year, we were able to develop a process for the synthesis of EC-359 so that large quantities can be synthesized efficiently.

The medicinal chemistry route for the preparation of EC-359 is shown in Scheme 1.

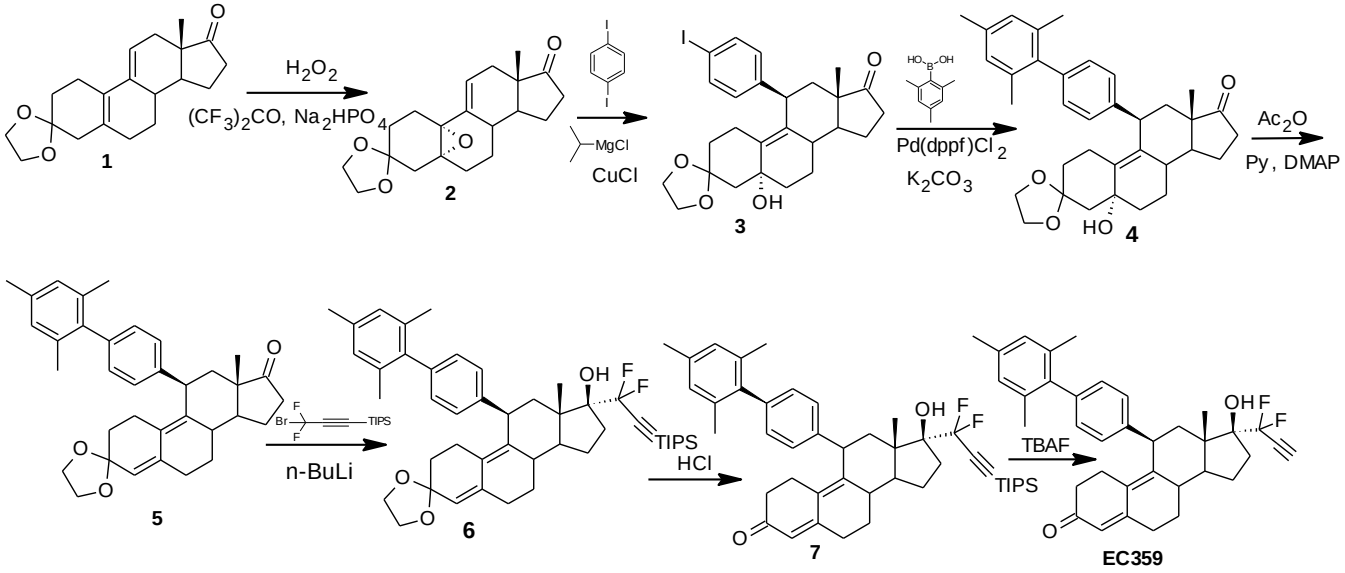

Scheme 1

The medicinal chemistry route consists of 7 steps and involve 5 chromatographic purifications. Moreover, it's lengthy, it involves the use of heavy metal such as palladium in the main synthetic scheme. The need for multiple chromatographies along the synthesis makes it very costly. The overall yield for EC-359 using the medicinal chemistry route was found to be only 28%.

To summarize the drawbacks of the above synthesis;

1. Long synthesis
2. Involve the use of a heavy metal such as palladium
3. Multiple chromatographies for purification.

Several synthetic routes were designed and tested for addressing the drawbacks and the route representing the most efficient and viable set of reactions are represented in scheme 2.

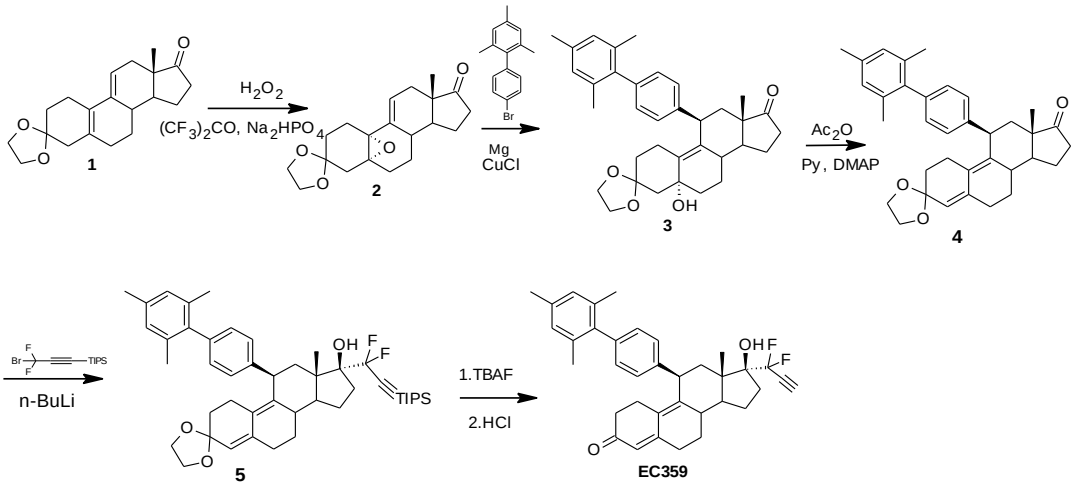

Scheme 2

All the synthetic steps shown in Scheme 2 has been optimized and it was proved to be the choice of the scheme toward the synthesis of EC359. As an outcome, enough quantities of EC359 with HPLC purity more than 98.5%, required for the preclinical *in vitro* and *in vivo* studies were prepared and made available for the biological studies at Vadlamudi lab. Process development for the large scale synthesis of EC359 is accomplished. Biological activity was tested using various TNBC models in vitro in Vadlamudi lab. The biological activity of EC359 correlated well with the original IC50 values of EC359. We will use this batch of EC359 mechanistic and preclinical studies proposed in year 2 and 3.

Multi-PI contributions: The above work was performed by Drs. Santhamma lab and Vadlamudi lab. Synthesis was done in Dr. Santhamma lab and the biological activity was tested in Vadlamudi lab.

Subtask2: To establish Absorption, Distribution, Metabolism, Excretion (ADME) of EC359 9 (Time line 1-24 months)

During the first year, we have completed ADME studies using CRO and results are summarized in figure 8. Ames test confirmed that EC359 did not induce an evident (significant) >2 fold increase in the revertant counts at the doses tested (dose related), with the tester strains both with and without metabolic activation according to the evaluation criteria mentioned in OECD guideline no.471. Hence, the compound EC359 is considered non-mutagenic with salmonella typhimurium strains TA98, TA100, TA1535, TA1537 and E.coli combo, both with and without metabolic activation. Among CYP enzymes EC359 inhibits 2D6 hence caution is warranted in concurrent administration that inhibits 2D6 such as Prozac. Metabolic stability and plasma stability are moderate in human with high plasma protein binding (Figure 18). Collectively, the data from these studies indicate EC359 as a druggable candidate for further development after establishing toxicology and safety pharmacology studies.

Compound	Assays	Result
EC359	Mutagenicity testing- S. typhimurium TA98, TA100, TA1535 and E.coli WP2 uvrA + E. coli WP2[pKM101] strains	No mutagenicity
EC359	Cardiotoxicity assessment (hERG): EC359 against hERG membrane using a fluorescence polarization assay	No liability
EC359	CYP inhibition: In vitro assessment of Cytochrome P450 Inhibition potential for EC359 using human liver microsomes (1A2, 2C9, 2C19, 2D6, 3A4)	2D6 inhibition
EC359	Hepatocyte stability: In vitro evaluation of EC359 compound for metabolic stability using cryopreserved human, mouse, rat and dog hepatocytes	Human & Mouse-moderate Rat & Dog - low
EC359	Microsomal stability: In vitro evaluation of EC359 compound for metabolic stability using cryopreserved human, mouse, rat and dog liver microsomes	Human & Mouse-moderate Rat & Dog- low
EC359	Plasma protein binding (%)	Human- 99.98; Mouse- 99.63; Rat- 99.89; Dog- 99.83
EC359	Plasma stability (% remaining at 60 min)	Human-113.92; Mouse- 104.91; Rat- 108.64; Dog- 105.61
EC359	Solubility: pION, kinetic, thermodynamic	Low <10 µg/mL
EC359	Metabolite identification	Major metabolic pathway- Phase I metabolism; No glucuronide metabolites as evidenced by low CL in UDPGA
EC359	Caco2 –permeability & efflux transporter substrate activity	Low permeable; No efflux transporter substrate activity
EC359	Off-target binding study (CEREP screen)	GR and hERG were identified as off targets, however, IC 50 of binding with these receptors - up to 10uM and 30uM no GR and hERG binding respectively
EC359	LIF and LIFR binding – Thermophoresis method	Kd LIFR- 10.2nM; Kd LIF- No binding up to 5microM

Figure 18. ADME studies of EC359

Multi-PI contributions: The above work was performed by Dr. Santhamma lab and Vadlamudi lab. ADME studies were completed by Dr. Santhamma with the help of CROs. Data analysis and interpretation was done in consultation with Dr. Vadlamudi lab.

Subtask3: Pharmacokinetic (PK) studies of EC359 in vivo (Time line 18-30 months)

In third year, we have completed the PK studies. The goal of these studies are to establish the time needed to obtain therapeutic drug concentration for EC359. We initially optimized the formulation for PK studies. Rats were used to treat orally with a single administration of EC359 formulated in a vehicle containing 58.5% Labrasol ALF, 22.5% Labrafil M, 1944 CS, 9% Capryol 90 and 10 % water q.s. at 0, 2.5, 5,15, 50, 100 and 300 mg/kg sequentially, based on the outcome of previous treatments. We then determined PK. These results showed that EC359 attained good systemic exposure following oral administration. Mean plasma clearance and mean volume of distribution/steady state showed that EC359 demonstrated very lower clearance suggesting 24 h interval may not be suitable for repeated dosing. Plasma half-life was found to be 4.5 h and this could be the reason for slower rate of elimination. Following intravenous bolus, EC359 eliminated as a biexponential decline. The results are summarized in Fig. 19 and Table 1.

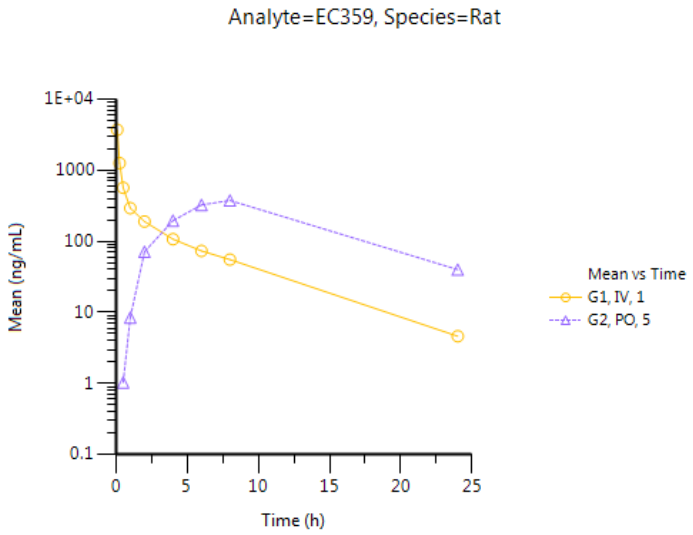

Figure 19. The PK study data and summary of the results.

Table 1. PK data for EC359.

C_0: Back extrapolated concentration at time zero; NR: Not reported due to improper elimination phase; @: Median

Treat	Group (Dose)	T_{max}@ (h)	C0/C_{max} (ng/mL)	AUC_{last} (ng.h/ mL)	AUC_{inf} (ng.h/ mL)	Cl (mL/ min/kg)	V_{ss} (L/kg)	V_d (L/kg)	$T_{1/2}$ (h)	%F	MRT (h)
EC 359	G1_IV (1 mg/kg)	NA	6469.44± 2531.87	2364.85± 204.03	2395.0± 210.85	7.0 ± 0.58	1.47 ± 0.17	2.71 ± 0.16	4.49 ± 0.28	-	3.17 ± 0.27
	G2-PO (5 mg/kg)	8	383.62 ± 220.66	3657.84 ± 1536.39	NR					**31**	10.51 ± 1.75

Subtask4: MTD and Toxicology Studies for EC359 (Time line 25-36 months)

During this reporting period, we have synthesized the 87 grams of EC359 in-house for MTD/DRF studies and preparing more API for the upcoming GLP-tox study requirements in rodent and non-rodent species. We have completed single Maximum Tolerable Dose (MTD) Study Followed by Repeated Dose (7 Days) Range Finding Study of EC359 in Sprague Dawley Rats. Routine cage-side observations were made for all animals once a day for general signs of toxicity (considering the peak period of anticipated effects after dosing) and twice a day to check morbidity and mortality. The rats were exposed to the test item at 0, 2.5, 5,15, 50, 100 and 300 mg/kg. The animals were weighed on the day of dosing and 48 h after dosing respectively. Blood was collected for clinical pathology investigations at pre-dose and on day 3 after each dose during the single dose phase of the study.

Clinical Signs: All animals treated at all dose levels survived the treatment and observation period. Animals treated at 0, 2.5 and 5 mg/kg, with a single oral dose of the test item were normal and were free from all visible clinical signs. Animals treated @ 15 mg/kg were dull following 1 h post treatment and persisted for around 2 hours. Dullness was observed in animals treated @ 50 and 100 mg/kg starting 1 h post treatment and continued till the end of the day. However, all animals were normal from post-treatment day 1 onwards. Animals treated @ 300 mg/kg were weak with abnormal gait and were lying prostrate starting 1 hour post-dose until 72 h post dose however, with little signs of recovery.

Body Weight (up to 300 mg/kg). Normal body weight gain was observed following treatment at around 48 h in animals treated up to 0, 2.5, 5,15 and 50 mg/kg as compared to respective pre-exposure weights. There was no body weight gain in animals treated @ 100 mg/kg. Animals treated @ 300 mg/kg revealed a marginal decrease (< 10%) in body weight following 48 h post dose.

Clinical Pathology (up to 300 mg/kg): No visible changes in the tested hematological and clinical chemistry parameters were observed in the samples collected after 72 hours as compared to pre-dose and control in animals treated at 0, 2.5, 5, 15, 50, 100 and 300 mg/kg.

Gross Pathology (up to 50 mg/kg): No abnormalities were detected during the gross pathological examination of animals treated at 0, 2.5,5, 15 and 50 mg/kg. The 100mg dose the animals were dull post-dose for 24 hours. The 300mg/kg dosed animals were dull for 4days to recover. Currently, we are analyzing hematological parameters to determine the repeated dose regimen for the MTD study.

3-3. What opportunities for training and professional development has the project provided?

During the third year, this project provided training opportunities for three fellows (two graduate students, one post-doctoral fellow). All the students/fellows were trained in conducting breast cancer research using BCa model cells, preclinical models, and interpreting the data. In addition, post-doctoral fellow was given opportunity to train graduate students; this provided an opportunity to sharpen their mentoring skills. All students were participated in weekly project meetings and presented their research once in a month as oral presentation. In addition, students/fellows were provided several professional development opportunities including participation in journal clubs, attendance of grand rounds, and attendance of ethics seminar series. Further, post doc and graduate students attended 2020 AACR SABCS annual meeting to present the research findings.

3-4. How were the results disseminated to communities of interest?

The third year study results were presented as a poster presentation in June 2020 AACR annual meeting.
A manuscript describing results from third year studies is currently in review in nature communication biology.

A manuscript describing the first year and second year results was published Molecular Cancer Therapeutics Journal 2019. PDF file attached at the end of the report.

3-5. What **do you plan to do during the next reporting period to accomplish the goals?**
During no cost extension period, we will complete ongoing signaling studies using TNBC xenograft tissues; will complete ongoing xenograft studies, complete needed biochemical assays for the manuscript in preparation and complete IHC studies, finish statistical analyses. We also aim to complete the ongoing *in vitro* toxicity assays for the IND application is underway at Eurofins Panlabs. The assays include, Ames fluctuation test, Bacterial cytotoxicity, Micronucleus Panel, Tumor Cell Proliferation Assay in P388D1 Mouse Lymphoma Cells.

4. IMPACT

4-1. What was the impact on the development of the principal discipline(s) of the project?

Our data demonstrated that EC359 is a highly potent LIFR inhibitor and demonstrated the specificity of EC359 for inhibition of LIF–LIFR interaction, confirmed the mechanism of action and on target specificity. EC359 also possesses favorable pharmacologic features. Our PDX tumor study demonstrated utility of EC359 in treating human TNBC tumors. Since EC359 is a small, stable molecule, it is amenable for translation to clinical trials.

4-2. What was the impact on other disciplines?

LIF and LIFR are over-expressed in multiple solid tumors. Considering the wide deregulation of LIF/LIFR axis in multiple tumors, a small molecule LIFR inhibitor EC359 may have utility in treating other solid tumors including ovarian cancer, colon cancer, and pancreatic cancer all which exhibit deregulated LIF/LIFR signaling.

4-3. What was the impact on technology transfer?
Nothing to Report.

4-4. What was the impact on society beyond science and technology?
Nothing to Report.

5. CHANGES/PROBLEMS

5-1. Changes in approach and reasons for change.
Nothing to Report.

5-2. Actual or anticipated problems or delays and actions or plans to resolve them
We experienced some delay in completing animal studies due to COVID related closures. However, these issues are resolved and remaining animal studies are in progress and will be completed during the no cost extension period without any anticipated problems or delays.

5-3. Changes that had a significant impact on expenditures
Nothing to Report.

5-4. Significant changes in use or care of human subjects, vertebrate animals, biohazards, and/or select agents
Nothing to Report.

6. PRODUCTS

6-1. Publications, conference papers, and presentations

1. Viswanadhapalli S, et al. Development of a first-in-class small molecule inhibitor (EC359) targeting oncogenic LIF/LIFR signaling for the treatment of triple negative breast cancer. Proceedings of San Antonio Breast Cancer Symposium. Poster Session 2: Tumor cell and molecular biology: Novel/Emerging Therapeutic Targets; Date/Time: Thursday, December 6, 2018 - 7:00 am. Poster #P2-06-02

2. Viswanadhapalli S, et al. Therapeutic utility of EC359 for targeting oncogenic LIFR signaling in triple negative breast cancer2019. *Proceedings of American Association for Cancer Research.*

3. Viswanadhapalli S, Luo Y, Sareddy GR, et al. EC359: A First-in-Class Small-Molecule Inhibitor for Targeting Oncogenic LIFR Signaling in Triple-Negative Breast Cancer. Mol Cancer Ther. 2019;18(8):1341–1354. doi:10.1158/1535-7163.MCT-18-1258

4. Viswanadhapalli S, et al. Development of a first-in-class small molecule inhibitor (EC359) targeting oncogenic LIF/LIFR signaling for the treatment of triple negative breast cancer. Proceedings of San Antonio Breast Cancer Symposium. Poster Session 2: Tumor cell and molecular biology: Novel/Emerging Therapeutic Targets; Date/Time: Thursday, December 6, 2018 - 7:00 am. Poster #P2-06-02.

5. Viswanadhapalli S, et al. Novel combination therapy for treating TNBC using LIFR and HDAC Inhibitors. Proceedings: AACR Annual Meeting 2020; April 27-28, 2020 and June 22-24, 2020; Philadelphia, PA. DOI: 10.1158/1538-7445.AM2020-562 Published August 2020.

6-2. Website(s) or other Internet site(s)

Nothing to Report.

6-3. Technologies or techniques
Nothing to Report.

6-4. Inventions, patent applications, and/or licenses
Nothing to Report.

6-5. Other Products
Nothing to Report.

7. PARTICIPANTS & OTHER COLLABORATING ORGANIZATIONS

7-1. What individuals have worked on the project?

Name	Project Role	Effort (mo.)	Site	Contribution to Project	Other Funding Support and Changes in the Reporting Period
Dr. Klaus Nickisch	Previous initiating PI	1.2	Evestra	Experiment design, project supervision, data analysis, Partner PI coordination, data presentation	**Active**: None to report
Dr. Bindu Santhamma	Initiating PI (current)	3.0	Evestra	Chemical synthesis, process development	1R44CA235991-01 (5.0 months)
Migdalis Cintron-Miguel	Co-Investigator	1.85	Evestra	Analytical method development, analytical measurements	None to report
Gulzar Ahmed	Co-Investigator	0.3	Evestra	Chemical synthesis, conjugation chemistry	1R44CA235991-01 (4.0 months)
Rebecca Huff	Administrative assistant	0.48	Evestra	Budgetary support	1R44CA235991-01 (1.5 months)
Angel Alcala	Administrative assistant	0.6	Evestra	Logistical support	1R44CA235991-01 (2.75 months)
Ratna Vadlamudi	Partner PI	1.36	UTHSCSA	Experiment design, project supervision, data analysis, Partner PI coordination, data presentation	R01CA223828(1.36 mo) DODBCRP:W81XWH-18-1-0016 (0.45 mo) R01CA239227-01 (0.72 mo) R56NS109908-01 (0.07mo) No cost extension 1R01NS106173-01A1 (0.6 mo)
Suryavathi Viswanad-hapalli	Post-doctoral fellow	4.8	UTHSCSA	Experiment design and execution, data analysis and presentation	Active: DOD BCRP :W81XWH-18-1-0021 (2.0 mo) The Elsa U. Pardee Foundation (4 mo)
Xaionan Li	Research Assistant	2.0	UTHSCSA	Experiment execution, data analysis and presentation	

7-2. Has there been a change in the active other support of the PD/PI(s) or senior/key personnel since the last reporting period?
Previous initiating PI, Dr. Klaus Nickisch retired from Evestra and he was replaced by Dr. Bindu Santhamma. This was approved by DOD.

7-3. What other organizations were involved as partners?
Nothing to Report.

8. SPECIAL REPORTING REQUIREMENTS

8-1. COLLABORATIVE AWARDS

This Progress Report is jointly authored by **Dr. Bindu Santhamma (Initiating PI)** and **Dr. Ratna Vadlamudi (Partner PI)** and provides details for the work performed in their respective laboratories. An identical copy of this Report will be submitted by Dr. Bindu Santhamma and Dr. Vadlamudi independently as their respective Progress Report.

8-2. Quad Chart

Not applicable.

9. APPENDICES

1) **[P2-06-02] Development of a first-in-class small molecule inhibitor (EC359) targeting oncogenic LIF/LIFR signaling for the treatment of triple negative breast cancer**

Authors: Viswanadhapalli S, Luo Y, Sareddy GR, Santhamma B, Zhou M, Li M, Pratap UP, Altwegg KA, Li X, Srinivasan U, Ma S, Chang A, Riveros AC, Zhang KY, Dileep KV, Pan X, Murali R, Bajda M, Raj G, Brenner A, Manthati V, Rao M, Tekmal RR, Nair HB, Nickisch KJ, Vadlamudi RK

Room: Hall 1

Date/Time: Thursday, December 6, 2018 - 7:00 am

Session Info: Poster Session 2: Tumor cell and molecular biology: Novel/Emerging Therapeutic Targets (7:00 AM-9:00 AM)

Development of a first-in-class small molecule inhibitor (EC359) targeting oncogenic LIF/LIFR signaling for the treatment of triple negative breast cancer

Viswanadhapalli S, Luo Y, Sareddy GR, Santhamma B, Zhou M, Li M, Pratap UP, Altwegg KA, Li X, Srinivasan U, Ma S, Chang A, Riveros AC, Zhang KY, Dileep KV, Pan X, Murali R, Bajda M, Raj G, Brenner A, Manthati V, Rao M, Tekmal RR, Nair HB, Nickisch KJ, Vadlamudi RK UT Health and Mays Cancer Center, San Antonio; Evestra, Inc., San Antonio; Instituto de Química, Ciudad de, Mexico; RIKEN Center for Biosystems Dynamics Research, Yokohama, Japan; Cidars-Sinai Medical Center, Los Angeles; Jagiellonian University, Cracow, Poland; UT Southwestern, Dallas

Background: Leukemia inhibitory factor (LIF) and its receptor LIFR are over-expressed in multiple solid tumors and play a key role in tumor growth, progression, and resistance to standard anti-cancer treatments. Triple-negative breast cancer (TNBC) lacks targeted therapies and represents a disproportional share of breast cancer (BCa) mortality. TNBC exhibits autocrine stimulation of the LIF/LIFR axis and overexpression of LIF is associated with poorer relapse-free survival in BCa patients. LIF signaling also promotes maintenance of stem cells. Therefore, targeting the LIF/LIFR axis may have therapeutic utility in TNBC.
Methods: We rationally designed a small organic molecule (EC359) that emulates the LIF/LIFR binding site and functions as a LIFR inhibitor from a library of compounds. *In silico* docking studies were used to identify the putative interaction of the EC359 and LIF/LIFR complex. Direct binding of EC359 to LIFR was confirmed using surface plasmon resonance (SPR) and microscale thermophoresis technique (MST) assays. *In vitro* activity was tested using Cell-Titer Glo, MTT, invasion, and apoptosis assays. Mechanistic studies were conducted using Western blot, reporter gene assays, and RNA-seq analysis. Xenograft, patient-derived xenograft (PDX), and patient-derived explant (PDEX) models were used for preclinical evaluation and toxicity.
Results: Molecular docking studies showed that EC359 interacts at the LIF/LIFR binding interface. SPR and MST studies confirmed direct interaction of EC359 to LIFR. EC359 reduced the growth of TNBC cells with high potency (IC50 50-100nM) and promoted apoptosis. Further, EC359 treatment reduced invasion and stemness of TNBC cells. EC359 activity is dependent on the expression levels of LIFR and showed little or no activity on TNBC cells that have low levels of LIFR or ER+ve BCa cells. Further, EC359 significantly reduced the viability of cisplatin and taxane-resistant TNBC cells and enhanced the efficacy of HDAC inhibitors. Mechanistic and biochemical studies showed that EC359 interacts with LIFR and effectively blocking LIF/LIFR interactions. EC359 also blocked LIFR interactions with other LIFR ligands such as oncostatin M, ciliary neurotrophic factor, and cardiotrophin-1. EC359 treatment attenuated the activation of LIF/LIFR driven pathways including STAT3, mTOR, AKT, and MAPK. RNA-seq analysis identified regulation of apoptosis as one of the important pathway modulated by EC359. In TNBC xenograft and PDX assays, EC359 significantly reduced tumor progression. Further, using human primary BCa PDEX cultures, we demonstrated that EC359 has the potential to substantially reduce the proliferation of human BCa. Pharmacologically, EC359 exhibited high oral bioavailability and long half-life with a wide therapeutic window.
Conclusions: EC359 is a novel targeted therapeutic agent that inhibits LIF/LIFR oncogenic signaling in TNBC via a unique mechanism of action**.** EC359 has the distinct pharmacologic advantages of oral bioavailability, *in vivo* stability, and is associated with minimal systemic side effects. (DOD BCRP grant #BC170312) **Session:** Poster Session 2: Tumor cell and molecular biology: Novel/Emerging Therapeutic Targets (7:00 AM-9:00 AM D**ate/Time:** Thursday, December 6, 2018 - 7:00am

Print this Page for Your Records Close Window

Control/Tracking Number: 19-A-3351-AACR
Activity: Abstract Submission
Current Date/Time: 11/14/2018 11:26:44 PM

Therapeutic utility of EC359 for targeting oncogenic LIFR signaling in triple negative breast cancer

Short Title:
LIFR therapy for breast cancer

Author Block: Suryavathi Viswanadhapalli[1], Mengxing Li[1], Yiliao Luo[1], Gangadhara R Sareddy[1], Bindu Santhamma[2], Mei Zhou[3], Shihong Ma[4], Rajni Sonavane[4], Uday P. Pratap[1], Kristin A. Altwegg[1], Annabel Chang[4], Alejandra Chávez-Riveros[5], Kalarickal V. Dileep[6], Kam Y. Zhang[6], Marek Bajda[7], Ganesh V. Raj[4], Andrew Brenner[1], Vijaya Manthati[2], Manjeet Rao[8], Rajeshwar R. Tekmal[1], Hareesh B. Nair[2], Klaus J. Nickisch[2], Ratna K. Vadlamudi[1]. [1]UT Health Science Ctr. at San Antonio, San Antonio, TX; [2]Evestra, Inc, San Antonio, TX; [3]Second Xiangya Hospital, San Antonio, TX; [4]UT Southwestern, Dallas, TX; [5]Instituto de Química, Mexico; [6]Center for Biosystems Dynamics Research, RIKEN, Yokohama, Japan; [7]Jagiellonian University Medical College, Cracow, Poland; [8]Greehey Children's Cancer Research Institute, San Antonio, TX

Abstract:
Background: Leukemia inhibitory factor receptor (LIFR) and its ligand LIF play a major critical role in cancer progression, metastasis, stem cell maintenance, and therapy resistance. Recent studies in breast cancer have shown that feedback activation of LIFR limits response to histone deacetylase (HDAC) inhibitors and induce resistance. We rationally designed a small molecule (EC359) that emulates the LIF-LIFR binding site and functions as a LIFR inhibitor from a library of compounds. Here, we tested the utility of EC359 as a monotherapy and to effectively block LIF-LIFR interactions in overcoming resistance to HDAC inhibitors.
Methods: We have used multiple triple negative breast cancer (TNBC) models that represent all six types of TNBC. *In vitro* activity was tested using Cell-Titer Glo, MTT, invasion, and apoptosis assays. Mechanistic studies were conducted using western blot, reporter gene assays, and RNA-seq analysis. Xenograft, patient-derived xenograft (PDX), and patient-derived explant (PDeX) models were used for preclinical evaluation and toxicity.
Results: EC359 treatment exhibited anti-proliferative effects, reduced invasiveness and stemness, and promoted apoptosis in all six TNBC cell lines. The activity of EC359 is dependent on LIF and LIFR expression and CRISPR mediated knockdown of LIFR significantly abolished EC359 activity. Treatment with EC359 attenuated the activation of LIF-LIFR driven pathways including STAT3, mTOR, and AKT. EC359 significantly reduced tumor progression in TNBC xenografts, PDX models and reduced proliferation in patient derived primary TNBC explants. In MTT based cell viability assays, addition of EC359 enhanced efficacy of SAHA compared to monotherapy of SAHA. In clonogenic survival assays, EC359 significantly enhanced ability of SAHA to reduce the colony formation compared to monotherapy. Mechanistic studies using three different TNBC models using western blot analysis and reporter gene assays confirmed activation of LIFR signaling pathway upon SAHA treatment and its blockage by EC359. Treatment of TNBC PDX explants with EC359 enhanced ability of SAHA to substantially decrease the proliferation (Ki-67 positivity) compared to monotherapy treated tumors.
Conclusions: Collectively, these data support EC359 as a novel targeted therapeutic that inhibits LIFR oncogenic signaling as a monotherapy or in combination with HDAC inhibitors.
:

Author Disclosure Information:

S. Viswanadhapalli: None. **M. Li:** None. **Y. Luo:** None. **G. Sareddy:** None. **B. Santhamma:** ; Evestra, Inc. **M. Zhou:** None. **S. Ma:** None. **R. Sonavane:** None. **U.P. Pratap:** None. **K.A. Altwegg:** None. **A. Chang:** None. **A. Chávez-Riveros:** None. **K.V. Dileep:** None. **K.Y. Zhang:** None. **M. Bajda:** None. **G.V. Raj:** None. **A. Brenner:** None. **V. Manthati:** ; Evestra, Inc. **M. Rao:** None. **R.R. Tekmal:** None. **H.B. Nair:** ; Evestra, Inc. **K.J. Nickisch:** ; Evestra, Inc. **R.K. Vadlamudi:** None.
Sponsor (Complete):
Category and Subclass (Complete): ET06-03 HDAC and methyltransferase inhibitors
Research Type (Complete): Translational research
Organ Site/Structures (Complete):
***Primary Organ Site:** Breast cancer
***Choose Chemical Structure Disclosure Option:**
YES, and I WILL DISCLOSE. Compounds with defined structures were used, and I WILL DISCLOSE them in my presentation.
***Please explain reason for not disclosing (maximum 250 characters with spaces):** : NA
***Reference or patent application number** : NA

Keywords/Indexing (Complete): Breast cancer ; Histone deacetylase inhibitor ; Small molecule inhibitor ; Signal transducers and activators of transcription (STAT)
Financial Support for Attendance (Complete):
Submission Fee (Complete): Your credit card order has been processed on Wednesday 14 November 2018 at 11:16 PM.
Status: Complete

***To log out, simply close your browser window. All information will be saved if you hit the Continue button after each step.

For all log-in problems or technical questions, please contact the OASIS Helpdesk or call (217) 398-1792.

(https://www.sabcs.org/2019-SABCS)
Session PS3 - PS3. Poster Session 3

Bookmark

Session PS3 - PS3. Poster Session 3

P3-11-08. Targeting LIFR enhances the activity of HDAC inhibitors for the treatment of triple negative breast cancer (https://www.sabcs.org/2019-SABCS)

December 12, 2019, 5:00 PM - 7:00 PM · Hall 1

Authors
Suryavathi Viswanadhapalli , Mengxing Li , Bindu Santhamma , Uday P Pratap , Yiliao Luo , Junhao Liu , Kristin A Altwegg , Xiaonan Li , Hui Yan , Zhenming Xu , Andrew Brenner , Gangadhara R Sareddy , Rajeshwar R Tekmal , Hareesh B Nair , Klaus J Nickisch and Ratna K Vadlamudi . UT Health San Antonio, San Antonio, TX; Evestra Inc., San Antonio, TX

Abstract
Background: Triple-negative breast cancer (TNBC) is a heterogeneous disease. TNBC lacks targeted therapies and represents a disproportional share of the breast cancer (BC) mortality rate. Histone deacetylase inhibitors (HDACIs) are emerging as promising multifunctional agents in TNBC to elicit cytotoxic actions. Recent studies have shown that cancer cells elucidate feedback activation of leukemia inhibitory factor receptor (LIFR) which in turn curtails response to HDACIs. We developed a first-in-class inhibitor of LIFR, EC359 that directly interacts with LIFR and effectively blocks LIFR downstream signaling. Here, we examined whether the novel LIFR inhibitor, EC359, has the ability to counteract negative effects of LIFR signaling to enhance HDACIs therapeutic efficacy in the treatment of TNBC.

Methods: We tested multiple HDACIs currently in clinical trials including vorinostat, panobinostat, romidepsin, and givinostat using multiple TNBC models. The effect of combination therapy of HDACIs and EC359 on TNBC cell viability and invasion was examined using MTT assays and matrigel invasion assays respectively. The e□cacy of combination therapy on cell survival and apoptosis was determined using clonogenic assays and Caspase 3/7 assays, respectively. Mechanistic studies were performed using Western blotting, qRT-PCR, and reporter gene assays. The efficacy of combination therapy *in vivo* was examined using Xenograft, patient-derived xenograft (PDX), and patient-derived explant (PDEX) models.

Results: We demonstrated that the treatment of TNBC models with HDACIs increased the expression of LIFR. Immunohistochemistry analyses of breast tumors using tissue microarrays revealed significant expression of LIFR in TNBC samples. Knockdown of LIFR or treatment with a small molecule inhibitor of LIFR (EC359) significantly enhanced the efficacy of HDACIs in reducing cell viability, colony formation ability, and invasiveness as well as promoted apoptosis compared to monotherapy of HDACIs or EC359 in TNBC cell lines. Mechanistic studies,
reporter gene assays and biochemical studies using multiple TNBC models exhibited activation of the LIFR signaling pathway upon HDACIs treatment but was attenuated by EC359+HDACI combination therapy. Treatment of human breast tumors utilizing PDEX assays showed that EC359 enhanced the ability of HDACIs to decrease the proliferation (Ki-67 positivity) compared to monotherapy. Furthermore, using TNBC xenografts and PDX models, we demonstrated that EC359 treatment enhanced the ability of HDACIs to reduce *in vivo* tumor growth compared to monotherapy.

Conclusions: Our results suggest that the combination therapy of HDACIs and EC359 provides greater therapeutic efficacy than monotherapy. In addition, treatment with EC359 can overcome the feedback activation of LIFR currently observed in the treatment of TNBC with HDACIs.

Abstract 562: Novel combination therapy for treating TNBC using LIFR and HDAC Inhibitors

Suryavathi Viswanadhapalli, Mengxing Li, Bindu Santhamma, Uday P. Pratap, Yiliao Luo, Junhao Liu, Kristin A. Altwegg, Xiaonan Li, Ahmed Gulzar, Hui Yan, Zhenming Xu, Andrew Brenner, Gangadhara R. Sareddy, Manjeet K. Rao, Rajeshwar R. Tekmal, Hareesh B. Nair, Klaus J. Nickisch and Ratna K. Vadlamudi

DOI: 10.1158/1538-7445.AM2020-562 Published August 2020
Proceedings: AACR Annual Meeting 2020; April 27-28, 2020 and June 22-24, 2020; Philadelphia, PA

Abstract

Background: Triple-negative breast cancer (TNBC) lacks targeted therapies and represents a disproportional share of the breast cancer (BC) mortality rate. TNBC exhibits autocrine stimulation of the LIF/LIFR axis and overexpression of LIF is associated with poorer relapse-free survival in BC patients. Histone deacetylase inhibitors (HDACIs) are emerging as promising multifunctional agents in TNBC to elicit cytotoxic actions. Recent studies have shown that cancer cells elicit feedback activation of leukemia inhibitory factor receptor (LIFR) which in turn curtails response to HDACIs. We developed a first-in-class inhibitor of LIFR, EC359 that directly interacts with LIFR and effectively blocks LIFR downstream signaling. The objective of this study is to examine the therapeutic efficacy of combination therapy using preclinical and patient-derived xenograft (PDX) models.
Methods: We tested utility of combination therapy using multiple HDACIs that are currently in clinical trails along with EC359. The effect of combination therapy was evaluated using MTT, invasion, colony formation, and Caspase3/7 assays. Mechanistic studies were performed using Western blotting, qRT-PCR, and STAT3 reporter assays. The efficacy of combination therapy *in vivo* was examined using xenograft, PDX, and patient-derived explant (PDEx) models.
Results: Immunohistochemical analyses of breast tumors using tissue microarrays revealed significant expression of LIFR in TNBC tissues. Treatment of TNBC model cells with four different HDACIs increased the expression of LIFR. LIFR inhibitor EC359 at nM concentration is additive to HDACIs in reducing cell viability. Knockdown of LIFR or treatment with EC359 significantly enhanced the efficacy of HDACIs in reducing the cell viability, colony formation ability, and invasiveness as well as promoted apoptosis compared to monotherapy in TNBC model cells. On the contrary, treatment with STAT3 inhibitor requires µM concentrations to reduce the cell viability of TNBC cells and is not additive to HDACIs. Mechanistic studies utilizing STAT3 reporter gene assays and biochemical studies using multiple TNBC model cells exhibited activation of the LIFR signaling pathway upon HDACIs treatment but was attenuated by EC359 therapy. Treatment of human TNBC utilizing PDEx assays showed that EC359 enhanced the ability of HDACIs to decrease proliferation (Ki-67 positivity) compared to monotherapy. Using TNBC xenografts and PDX models, we demonstrated that EC359 treatment enhanced the ability of HDACIs to reduce *in vivo* tumor growth compared to monotherapy.
Conclusions: Our results suggest that the combination therapy of HDACIs and EC359 provides therapeutic utility in overcoming the limitation of feedback activation of LIFR observed in the treatment of HDACIs in treating TNBC. Supported by DOD BCRP grant W81XWH-18-1-0016 (R.K. Vadlamudi; K.J. Nickisch)
Citation Format: Suryavathi Viswanadhapalli, Mengxing Li, Bindu Santhamma, Uday P. Pratap, Yiliao Luo, Junhao Liu, Kristin A. Altwegg, Xiaonan Li, Ahmed Gulzar, Hui Yan, Zhenming Xu, Andrew Brenner, Gangadhara R. Sareddy, Manjeet K. Rao, Rajeshwar R. Tekmal, Hareesh B. Nair, Klaus J. Nickisch, Ratna K. Vadlamudi. Novel combination therapy for treating TNBC using LIFR and HDAC Inhibitors [abstract]. In: Proceedings of the Annual Meeting of the American Association for Cancer Research 2020; 2020 Apr 27-28 and Jun 22-24. Philadelphia (PA): AACR; Cancer Res 2020;80(16 Suppl):Abstract nr 562.

Published OnlineFirst May 29, 2019; DOI: 10.1158/1535-7163.MCT-18-1258

Molecular Cancer Therapeutics

EC359: A First-in-Class Small-Molecule Inhibitor for Targeting Oncogenic LIFR Signaling in Triple-Negative Breast Cancer

Suryavathi Viswanadhapalli[1], Yiliao Luo[1,2], Gangadhara R. Sareddy[1,3], Bindu Santhamma[4], Mei Zhou[1,5], Mengxing Li[1,6], Shihong Ma[7], Rajni Sonavane[7], Uday P. Pratap[1], Kristin A. Altwegg[1], Xiaonan Li[1], Annabel Chang[7], Alejandra Chávez-Riveros[4], Kalarickal V. Dileep[8], Kam Y.J. Zhang[8], Xinlei Pan[9], Ramachandran Murali[9], Marek Bajda[10], Ganesh V. Raj[7], Andrew J. Brenner[3,11], Vijaya Manthati[4], Manjeet K. Rao[3,12], Rajeshwar R. Tekmal[1,3], Hareesh B. Nair[4], Klaus J. Nickisch[4], and Ratna K. Vadlamudi[1,3]

Abstract

Leukemia inhibitory factor receptor (LIFR) and its ligand LIF play a critical role in cancer progression, metastasis, stem cell maintenance, and therapy resistance. Here, we describe a rationally designed first-in-class inhibitor of LIFR, EC359, which directly interacts with LIFR to effectively block LIF/LIFR interactions. EC359 treatment exhibits antiproliferative effects, reduces invasiveness and stemness, and promotes apoptosis in triple-negative breast cancer (TNBC) cell lines. The activity of EC359 is dependent on LIF and LIFR expression, and treatment with EC359 attenuated the activation of LIF/LIFR-driven pathways, including STAT3, mTOR, and AKT. Concomitantly, EC359 was also effective in blocking signaling by other LIFR ligands (CTF1, CNTF, and OSM) that interact at LIF/LIFR interface. EC359 significantly reduced tumor progression in TNBC xenografts and patient-derived xenografts (PDX), and reduced proliferation in patient-derived primary TNBC explants. EC359 exhibits distinct pharmacologic advantages, including oral bioavailability, and *in vivo* stability. Collectively, these data support EC359 as a novel targeted therapeutic that inhibits LIFR oncogenic signaling.

See related commentary by Shi et al., p. 1337

Introduction

Leukemia inhibitory factor (LIF) is the most pleiotropic member of the IL6 family of cytokines (1). LIF signaling is mediated via the LIF receptor (LIFR) complex, which is comprised of LIFR and glycoprotein 130 (gp130; ref. 2). The LIFR does not have intrinsic tyrosine kinase activity. Both LIFR and gp130 constitutively associate with the JAK–Tyk family of cytoplasmic tyrosine kinases. Consequently, LIF binding to the LIFR complex activates multiple signaling pathways, including JAK/STAT, MAPK, AKT, and mTOR (2–4). LIF and LIFR are widely expressed in many solid tumors (1, 5–7) and their overexpression is often associated with poor patient prognosis (8, 9). In addition, high circulating LIF levels correlate with tumor recurrence (10).

The LIF/LIFR axis acts on multiple aspects of cancer biology to promote tumor growth, metastasis, and therapy resistance (11). LIF is a key regulator of cancer stem cells (CSC; ref. 11), plays a role in stem cell maintenance (12, 13), regulates self-renewal and pluripotency (12), and is associated with chemoresistance (10, 14). LIF functions as a growth factor to promote growth and invasion (15). Recent evidence indicates upregulated LIF–JAK–STAT3 signaling via autocrine and paracrine mechanisms in tumors (10, 16, 17). However, lack of any small-molecule inhibitors (SMI) that block LIF/LIFR signaling represents a major knowledge gap and critical barrier for advancement of LIF/LIFR–targeted cancer therapy.

Among the different subtypes of breast cancer, 60%–70% are estrogen receptor (ER) positive (ER^+ breast cancer), and 15%–24% are triple-negative breast cancer (TNBC; ref. 18). TNBC is more aggressive, and due to the lack of targeted therapies, represents a disproportional share of the breast cancer mortality (19, 20). TNBC exhibit high propensity for metastasis, with some subtypes such as claudin-low that are highly enriched for

[1]Department of Obstetrics and Gynecology, University of Texas Health San Antonio, San Antonio, Texas. [2]Department of General Surgery, Xiangya Hospital, Hunan, China. [3]Mays Cancer Center, University of Texas Health San Antonio, San Antonio, Texas. [4]Evestra, Inc., San Antonio, Texas. [5]Department of Gastroenterology, Second Xiangya Hospital, Hunan, China. [6]Department of Respiratory Medicine, Xiangya Hospital, Central South University, Hunan, China. [7]UT Southwestern Medical Center, Dallas, Texas. [8]Laboratory for Structural Bioinformatics, Center for Biosystems Dynamics Research, RIKEN, Yokohama, Kanagawa, Japan. [9]Cedars-Sinai Medical Center, Los Angeles, California. [10]Jagiellonian University Medical College, Krakow, Poland. [11]Hematology & Oncology, University of Texas Health San Antonio, San Antonio, Texas. [12]Greehey Children's Cancer Research Institute, University of Texas Health San Antonio, San Antonio, Texas.

Note: Supplementary data for this article are available at Molecular Cancer Therapeutics Online (http://mct.aacrjournals.org/).

Current address for A. Chávez-Riveros: Department of Medicinal Chemistry, University of Florida, Miami, Florida.

Corresponding Authors: Ratna K Vadlamudi, University of Texas Health San Antonio, 7703 Floyd Curl Drive, San Antonio, TX 78229. Phone: 210-567-4930; Fax: 210-567-4958; E-mail: vadlamudi@uthscsa.edu; and Hareesh B. Nair, Evestra, Inc., 14805 Omicron Drive, San Antonio, TX 78245. Phone: 210-278-9819; E-mail: hnair@evestra.com

Mol Cancer Ther 2019;18:1341–54

doi: 10.1158/1535-7163.MCT-18-1258

Published OnlineFirst May 29, 2019; DOI: 10.1158/1535-7163.MCT-18-1258

CSCs, and frequently exhibits therapy resistance (19, 20). In breast cancer cells, LIF/LIFR signaling activates multiple signaling pathways including STAT3, AKT, and mTOR pathways and contributes to activation of mTOR downstream targets such as p70S6K and 4EBP1 (4). LIF/LIFR signaling promote tumor progression of both ER^+ breast cancer and TNBC cells (21–23). In addition, LIF mRNA levels were elevated in invasive breast carcinomas compared with the normal breast tissues (24). Overexpression of LIF is significantly associated with a poorer relapse-free survival in patients with breast cancer (4).

In this study, we report the development of a novel LIFR inhibitor EC359 that selectively binds LIFR and blocks binding of ligands attenuating LIFR oncogenic signaling. Using molecular modeling, *in vitro*, and *in vivo* assays, we demonstrated that EC359 interacts with LIFR and inhibits cell viability of TNBC cells that express both LIF and LIFR. In addition, EC359 reduced the invasion and stemness of TNBC cells, and promoted apoptosis. In xenograft and patient-derived xenograft (PDX) assays, EC359 significantly reduced the tumor progression. This study represents the first report detailing the development of a first-in-class inhibitor of LIF/LIFR.

Materials and Methods

Cell lines and reagents

Human breast cancer cells MCF7, T47D, MDA-MB-231, BT-549, SUM-159, HCC1937, MDA-MB-468, HCC1806, and normal mammary epithelial cells (HMEC) were obtained from ATCC, were maintained as per ATCC guidelines, and used from early passages (<10 passages after thawing). All model cells utilized were free of *Mycoplasma* contamination and were confirmed by using the Mycoplasma PCR Detection Kit purchased from Sigma. Short tandem repeat polymorphism analysis of the cells was used to confirm the identity at University of Texas Health San Antonio (UTHSA) core facilities. CSCs isolated from TNBC cells were maintained in MammoCult medium along with the supplements according to the manufacturer's instructions (StemCell Technologies). The GAPDH, p-ERK1/2, ERK1/2, p-p70S6K, p70S6K, p-S6, S6, p-Akt(S473), Akt, p-p38 MAPK, p38 MAPK, p-mTOR(S2448), mTOR, p-STAT3(Y705), and STAT3 antibodies were purchased from Cell Signaling Technology. LIF and LIFR antibodies were purchased from Santa Cruz Biotechnology. β-Actin and all secondary antibodies were purchased from Sigma. ALDEFLUOR assay kit was obtained from StemCell Technologies. The Ki-67 antibody was purchased from Abcam. LIFR Knockout (KO) model cells were generated using Genescript CRISPR gRNA Constructs (Genescript-s64729-LIFR CRISPR guide RNA 1; Genescript-s64731-LIFR CRISPR guide RNA 2) and transfecting them into Cas9 stably expressing BT-549 cells followed by puromycin selection. EC359 and EC330 were synthesized using the detailed synthetic protocol described in the patent WO 2016/154203 A1 (Evestra Inc.). Characterization of EC330 and EC359 produced was described in the Supplementary Methods.

Western blotting and biotin pull-down assays

For Western blotting, cells were lysed in RIPA buffer (Thermo Fisher Scientific) containing protease and phosphatase inhibitors. Total cellular lysates were mixed with 4× SDS sample buffer and run on SDS-PAGE, and transferred onto nitrocellulose membranes and blots were developed using antibodies and the ECL Kit (Thermo Fisher Scientific). Avidin-biotin pull down was performed as described previously (25). Briefly, BT-549 total cellular lysates and purified LIFR was incubated with Biotin-control or Biotin-EC359 overnight and incubated with NanoLink Streptavidin Magnetic Beads (Solulink) for 1 hour at room temperature. The binding of EC359 to LIFR was confirmed by Western blotting. Intensity of signaling bands in Western blots were quantitated using ImageJ program (NIH, Bethesda, MD).

Cell invasion assays

The effect of EC359 on cell invasion of TNBC cells was determined by using the Corning BioCoat Growth Factor Reduced Matrigel Invasion Chamber assay. MDA-MB-231 and BT-549 cells were treated with vehicle or EC359 (25 nmol/L) for 22 hours and invaded cells in all the treatment conditions were determined according to the manufacturer's protocols.

Extreme limiting dilution assays

CSCs from MDA-MB-231 and BT-549 cells were sorted using established stem cell marker ALDH using the ALDEFLUOR kit and flow cytometry. CSCs were cultured in MammoCult medium with the supplements as per manufacturer's instructions. The effect of EC359 on self-renewal of CSCs was determined by ELDA. Briefly, CSCs were seeded in decreasing numbers (100, 50, 20, 10, 5, and 1 cells/well) in 96 well ultra-low attachment plates and treated with vehicle or EC359. After 10 days, the number of wells containing spheres per each plating density was recorded and stem cell frequency between control and treatment groups was calculated using ELDA analysis software (http://bioinf.wehi.edu.au/software/elda/).

Cell viability, clonogenic, and apoptosis assays

The effect of EC359 on cell viability of TNBC cells was assessed by using MTT assay as described previously (25). TNBC cells were seeded in 96-well plates (1×10^3 cells/well) and after overnight incubation cells were treated with varying concentrations of EC359 for 5 days. To test the effect of EC359 on the viability of CSCs and non CSCs, CellTiter-Glo assays were performed (Promega). Briefly, cells were seeded in 96-well, flat, clear-bottom, opaque-wall microplates and treated with vehicle or EC359 for 3 days. The total ATP content as an estimate of total number of viable cells was measured on an automatic Fluoroskan Luminometer. For clonogenic survival assays, cells were seeded in triplicates in 6-well plates (500 cells/well), after overnight incubation cells were treated with vehicle or EC359 for 5 days and after 2 weeks, colonies that contain $\geq$ 50 cells were counted and used in the analysis. The effect of EC359 on apoptosis was measured by Annexin V/PI staining and Caspase-3/7 activity assay as described previously (25, 26). Briefly, MDA-MB-231 and BT-549 cells were seeded in 96-well plates (2×10^3/well), after overnight incubation cells were treated with vehicle or EC359 (20 nmol/L) for 72 hours. After treatment, equal amount of caspase-3/7 substrate containing solution was added to the media, and luciferase activity was measured using luminometer according to the manufacturer's protocol (Promega).

qRT-PCR

Reverse transcription (RT) reactions were performed by using SuperScript III First Strand kit (Invitrogen), according to the manufacturer's protocol. Real-time PCR was done using Sybr-Green on an Illumina Real-Time PCR system. Primer sequences were included in the Supplementary Table S1.

Published OnlineFirst May 29, 2019; DOI: 10.1158/1535-7163.MCT-18-1258

Surface plasmon resonance studies

Binding profiles of EC359 to LIF/LIFR were evaluated using surface plasmon resonance (SPR). Recombinant human LIF was purchased from R&D Systems (catalog no. 7734-LF-500) and human LIFR-Fc was purchased from Speed Biosystems (catalog no. YCP1132). Sensor chips were purchased from ForteBio (www.fortbio.com). Detailed SPR protocol was provided in the Supplementary Methods.

Microscale thermophoresis assays

A serial dilution of the ligand (EC359) was prepared in a way to match the final buffer conditions in the reaction mix (10 mmol/L HEPES pH 7.4, 150 mmol/L NaCl, 3 mmol/L EDTA, 0.005 % Tween-20, 10% DMSO). The highest concentration of ligand was 2.00 μmol/L and the lowest 61.0 pmol/L. Five microliters of each dilution step was mixed with 5 μL of the fluorescent molecule. The final reaction mixture, which was loaded in capillaries, contained a respective amount of ligand (max. conc: 1.00 μmol/L; min. conc: 30.5 pmol/L) and constant 5 nmol/L fluorescent molecule (protein target LIFR-labeled fluorescent dye- NHS chemistry). Thermophoretic movement of fluorescently labeled protein with EC359 was performed using on a Monolith NT.115 Pico at 25°C, with 7% LED power and 60% Laser power (Nanotemper Technologies).

Molecular modeling studies

The atomic level interactions of EC359 against human LIFR (hLIFR) were studied by molecular modeling. The existing structural information of LIFR was utilized for the studies. The partial structure of human LIFR (hLIFR; domains D1–D5; PDB ID: 3E0G) and the structure of human LIF (hLIF) in complex with the partial murine LIFR (mLIFR; domains D1–D5) have been reported in the Protein Data Bank (PDB ID: 2Q7N; refs. 27, 28). As a preliminary step, the sequence and structural similarities of both of these LIFRs were deduced. Furthermore, the three-dimensional structure of hLIF–hLIFR complex was constructed from hLIF-mLIFR by replacing mLIFR. The complex was energy minimized to avoid the residue clashes between the hLIFR and hLIF. From the minimized complex, the hLIFR was again separated and prepared for the docking studies. Because there was no information available on the ligand-binding sites, the whole receptor was probed using Sitemap (Schrödinger) to detect possible binding sites (29). Two steps of molecular docking were performed such as standard precision (SP) and induced fit (IFD) on the identified binding sites. The purpose of SP docking was to detect the binding strength and orientations of ligand at respective binding sites. On the basis of the docking scores, the sites were ranked. Later, an appropriate ligand pose was selected and flexible docking (IFD) was performed by allowing flexibility to the surrounding amino acids (around 6 Å from the center of the ligand). On the basis of the MM-GBSA (30) score and visual inspection an appropriate pose was selected and subjected to molecular dynamics simulation (MDS) to estimate the residence time of the ligand over a period of 25 nanoseconds. The detailed description of methods used in the study was included in the Supplementary Methods and Supplementary Figs. S2 and S3.

Reporter gene assays

For STAT3-luc assays, MDA-MB-231 and BT-549 cells were stably transduced with STAT3-firefly luciferase reporter lentivirus purchased from Cellomic Technology. STAT3-luc reporter–expressing cells were serum starved for 24 hours, pretreated with EC359 for 1 hour, and then stimulated with LIF or other indicated ligands for 24 hours. Cells were lysed in passive lysis buffer, and the luciferase activity was measured by using the dual-luciferase reporter assay system (Promega) using luminometer.

In vivo xenograft studies

All animal experiments were performed after obtaining University of Texas Health San Antonio (UTHSA) Institutional Animal Care and Use Committee (IACUC) approval, and all the methods were carried out in accordance with IACUC guidelines. MDA-MB-231 cells (2×10^6) were mixed with equal volume of growth factor–reduced Matrigel and implanted in the mammary fat pads of 8-week-old female athymic nude mice as described previously (31). After tumor establishment, and achievement of measurable size, mice were randomized into control and treatment groups ($n = 8$ tumors per group). Control group received vehicle (hydroxymethylcellulose) and the treatment group received EC359 (5 mg/kg/day) 3 days per week subcutaneously. All mice were monitored daily for adverse toxic effects. Tumor growth was measured with a caliper at 3–4 day intervals, and volume was calculated using a modified ellipsoidal formula: tumor volume $= 1/2(L \times W^2)$, where L is the longitudinal diameter and W is the transverse diameter. At the end of the experiment, mice were euthanized, and tumors were excised, and processed for histologic and biochemical studies.

Patient-derived xenograft model

The TNBC tissue was obtained from a deidentified surgical specimen (F0) just after surgery from a patient with invasive ductal carcinoma (pT3 pN2a pM) via UTHSA PDX Core. The tumor tissues were divided in to three parts; the first part was snap frozen and stored in liquid nitrogen, the second part was fixed in 10% buffered formalin and processed for histologic characterization, and the third part was placed in ice-cold PBS, cut into small pieces (3–5mm^3), and engrafted into mammary fat pad of NCI SCID/NCr mice. PDX tumor was confirmed negative for ER, PR, HER2 by the Pathology core. Tumors from early passages were dissected into small pieces and implanted into the flanks of SCID mice. The mice were then randomized when they reached tumor volume of approximately 150 mm^3 into control or treatment groups ($n = 6$ tumors per group). The control group received vehicle (hydroxymethylcellulose) and the treatment group received EC359 (10 mg/kg/day) 3 days per week subcutaneously. At the end of the treatment, tumors were excised and processed for histologic studies, protein, and RNA analysis.

Patient-derived explant studies

TNBC tissues were collected from discarded surgical samples from UT Southwestern Medical Center (UTSW, Dallas, TX) patients for research purposes after obtaining the written informed consent and in accordance with institutional review board–approved protocol (STU-032011–187). All the studies were conducted in accordance with the Declaration of Helsinki. Tissues were processed and excised into small pieces and cultured on gelatin sponges for 24 hours in medium containing 10% FBS as described previously (25). Tissues were treated with vehicle or EC359 in culture medium for 72 hours and fixed in 10% buffered formalin at 4°C overnight and subsequently processed into

Published OnlineFirst May 29, 2019; DOI: 10.1158/1535-7163.MCT-18-1258

paraffin blocks. Sections were then processed for IHC analysis for Ki-67.

Immunohistochemistry (IHC)

IHC analysis was performed as described previously (25). Briefly, sections were blocked with normal goat serum (Vector Laboratories) followed by incubation overnight with Ki-67 (1:100) primary antibody and subsequent secondary antibody incubation for 30 minutes at room temperature. Immunoreactivity was visualized by using the DAB substrate and counterstained with hematoxylin (Vector Laboratories). Percent of Ki-67–positive proliferating cells was calculated in five randomly selected microscopic fields.

Pharmacokinetic studies and bioavailability studies

A pharmacokinetic study of EC359 was conducted in both mice and rats following intravenous and oral administration of the compound (GVK Bio). Intravenous formulation (5 mg/kg) was prepared as described: A required volume 0.1 mL of DMSO stock (20 mg/mL) was taken in an Eppendorf tube then 0.100 mL of DMSO was added and vortexed, then sonicated, followed by addition of 1.800 mL 10% Solutol in PBS, vortexed, and probe sonicated approximately 1–2 minutes to make a final solution of 1 mg/mL concentration. $t_{1/2}$, $AUC_{0\text{-last}}$, $AUC_{0\text{-inf}}$, AUC_{extra}, CL, Vd, $MRT_{0\text{-last}}$, and RSQ were measured using LC/MS-MS. For oral dosing (10 mg/kg) volume, 0.200 mL of DMSO stock (20 mg/mL) was taken in an Eppendorf tube then 1.800 mL 10% Solutol in PBS was added, vortexed, and probe sonicated approximately 1–2 minutes to make a solution of 2 mg/mL concentration. C_{max}, T_{max}, $AUC_{0\text{-last}}$, $AUC_{0\text{-inf}}$, AUC_{extra}, F%, $MRT_{0\text{-last}}$, and RSQ were measured. GR antagonism assays were performed using SelectScreen Biochemical Nuclear Receptor Profiling Service (Invitrogen).

Statistical analysis

All the statistical analyses were carried out using GraphPad Prism 6 software (GraphPad Software). A Student *t* test was used to assess statistical differences between control and EC359-treated groups. All the data represented in bar graphs are shown as mean ± SE. A P less than 0.05 was considered significant.

Data and materials availability

All data supporting the conclusions are included in the paper and/or in the Supplementary Materials.

Results

Optimization and generation of lead LIFR inhibitor EC359

We initially synthesized several compounds to target LIFR signaling using rationalized design based on crystal structure of LIF/LIFR. Within this series of compounds, one compound (EC330) showed higher potency (Fig. 1A, left). In cell viability assays (CellTiter Glo luminescent assay) using cancer cells, EC330 inhibited growth at approximately $IC_{50} \sim 50$ nmol/L (Fig. 1B). The reported X-ray crystallographic studies of LIF suggested a four α-helix bundle topology with a compact core predominantly composed of hydrophobic residues contributed by the four α-helices (32). Initial structure–activity relationship studies in our laboratory have shown the following structural features are necessary for the LIF inhibitory action: (i) difluro-acetylenic function at the 17-alpha position and (ii) 4′-substituition at the 11-phenyl ring. Because the EC330 has a steroidal backbone, we investigated the binding of EC330 to steroid receptors such as glucocorticoid receptor (GR). EC330 showed some antagonism to GR (79.8 nmol/L), which may elicit unwanted toxicity. Therefore, we pursued medicinal chemistry modifications, which retained its potency on LIFR, while reduced steroidal–receptor interactions. Additional SPR studies and subsequent synthetic efforts resulted in the development of EC359 (Fig. 1A, right). To examine whether optimization of EC359 retained its activity on par with the initial lead compound EC330, we conducted several studies. Receptor-binding studies revealed EC359 has more desirable characteristics than EC330 including lack of affinity to GR (Fig. 1C). In cell viability assays, EC359 showed significant inhibitory activity on par with EC330 in BT-549 model cells (Fig. 1B).

SPR studies confirmed EC359 direct interaction with LIFR

To test whether EC359 directly bind to LIFR complex, binding profiles of EC359 to LIF/LIFR were evaluated using SPR. Two sets of studies were performed: (i) to verify the integrity of recombinant proteins, the interaction between LIFR and LIF was studied; (ii) small-molecule binding to LIF/LIFR by either immobilizing LIFR or LIF onto a sensor chip was tested. Results from the first set of studies confirmed the integrity of recombinant LIF and LIFR; LIF bound to immobilized LIFR-Fc with a binding constant of 7 μmol/L (Supplementary Fig. S1A). In the second set of studies, results showed EC359 binding to LIFR, but not LIF. Furthermore, EC359 bound to LIFR in a dose-dependent manner with $K_d = 81$ μmol/L (Supplementary Fig. S1B). The results confirmed that EC359 is a specific inhibitor of LIF/LIFR complex.

MST assays revealed high-affinity interaction of EC359 with LIFR

Ligand binding to the immobilized receptor in SPR technique will be insensitive to ligand-induced structural changes, and thus the measured affinity by SPR may obscure true (*in vivo* equivalent) affinity of the drug. Hence, we conducted an orthogonal assay, namely MST, where the receptor is not immobilized to verify EC359 binding to the receptor complex. MST is a powerful technique to quantify biomolecular interactions. By combining the precision of fluorescence detection with the variability and sensitivity of thermophoresis, MST provides a flexible, robust, and fast way to dissect molecular interactions (33, 34). MST analysis confirmed direct interaction of EC359 with LIFR with an estimated K_d of 10.2 nmol/L (Fig. 1D). To further demonstrate that EC359 directly interacts with LIFR, we generated biotinylated EC359. Biotin addition did not affected EC359 biological activity (Supplementary Fig. S1C). Using biotin-EC359, we examined whether it interacts with LIFR. Purified LIFR protein or BT-549 cellular lysate was incubated with biotin-EC359 and its ability to interact with LIFR was determined using avidin pull-down assay followed by Western blotting. Results elucidated that EC359 interacts with LIFR (Supplementary Fig. S1D and S1E).

Docking studies suggested EC359 can interact at the LIF–LIFR binding interface

The site predictions revealed five potential binding sites on the hLIFR (Supplementary Fig. S4) in which two sites (2 and 3) are close to the LIF-binding interface (Supplementary Fig. S4). The SP docking was performed on all the five sites and docking scores were deduced (Fig. 1EA). The docking scores toward different

Published OnlineFirst May 29, 2019; DOI: 10.1158/1535-7163.MCT-18-1258

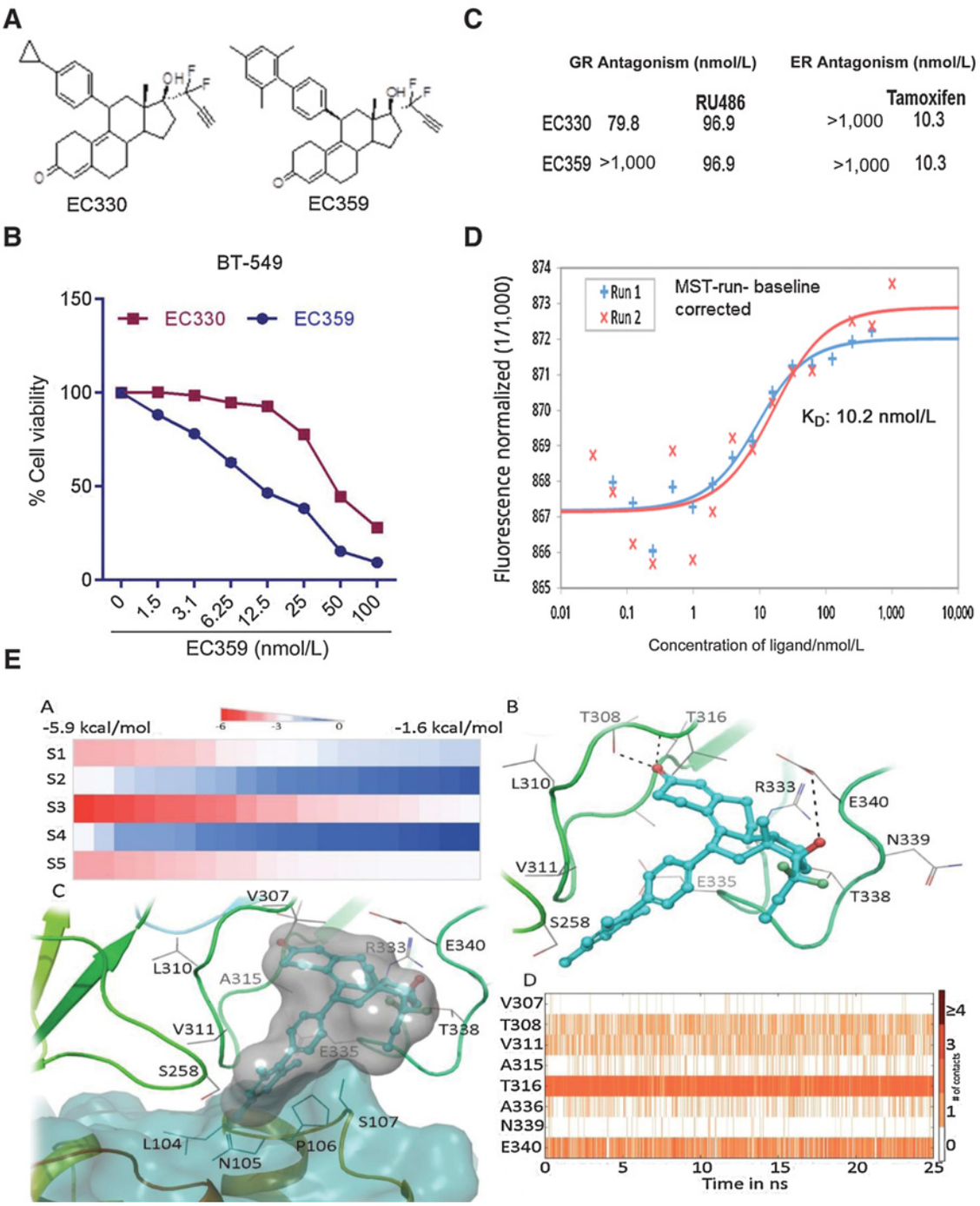

Figure 1.

Characterization of EC359. **A,** Schematic representation of the structure of EC330 and EC359. **B,** Dose–response curve of EC330 and EC359 determined using MTT assay on BT-549 cells ($n = 3$). **C,** Ability of EC359 to interact with other steroid receptors was analyzed by *in vitro* binding assays. **D,** Binding of EC359 to LIFR was confirmed using MST assays as described in Materials and Methods. **E**A, The docking scores of EC359 at different binding sites. The sites were mentioned as S1 to S5. **E**B, Binding of EC359 (represented in blue ball and stick model) with hLIFR (represented in cartoon and line model). The dotted lines represent the hydrogen bonds. **E**C, The binding of EC359 in the presence of LIF (represented in blue surface). The binding creates close contacts with residues of LIF. **E**D, The protein ligand contacts over 25 nanoseconds of MD.

Published OnlineFirst May 29, 2019; DOI: 10.1158/1535-7163.MCT-18-1258

binding sites range from -5.8 to -1.6 kcal/mol. It was also observed that EC359 has exhibited more promising scores toward site-3 compared with other sites. The binding poses obtained from the docking were superimposed to the hLIF–hLIFR complex to see the potential clashes between the ligand and LIF. As expected, the binding poses at site-3 are making steric clashes with residues of LIF (Supplementary Fig. S5). Because the SP docking is a rigid docking method, the ligand-induced conformational changes were also studied using IFD by applying flexibility to the surrounding residues. Using standard protocol, the side chains were optimized and 28 poses were generated. The binding energies of all the 28 poses range from -80 kcal/mol to -33 kcal/mol (Supplementary Fig. S6). It was observed that all the generated ligand poses are potentially making steric clashes with hLIF. One of the top scored poses (binding energy = -77 kcal/mol) was critically analyzed for the detailed atomic level interactions (Fig. 1EB). In the selected pose, ligand-induced conformational changes were observed for the loops close to the LIF-binding region (Supplementary Fig. S7). The ligand EC359 was found to sandwich between two loops at the N-terminal of D4 domain by orienting the difluro-acetylenic group to the bulk solvent. The keto group of the EC359 was found to be involved in two hydrogen bonds with the side chain of T308 and the backbone of T316. Similarly, the hydroxyl group of the ligand was also found to mediate a hydrogen bond with the sidechain of E340. Moreover, van der Waals contacts with the surrounding residues were also found to contribute to the ligand binding. It was observed that EC359 binding to hLIFR would prevent hLIF binding due to steric clashes (Fig. 1EC). As a final step, the snapshots obtained from the MD simulation were superimposed with the initial pose and RMSD was calculated for protein and ligand separately. The snapshots were analyzed and found that the structural distortions are affected mainly to the loops (connecting separate domains in the LIFR) and the terminal regions. At the same time the ligand is found to remain bound at the binding site even after 25 nanoseconds of MD simulation. The protein ligand contacts over 25 nanoseconds of MD simulation are shown in (Fig. 1ED; Supplementary Fig. S8).

EC359 has favorable pharmacologic features

We then conducted pharmacokinetic analysis of EC359 using various established tests (Supplementary Fig. S9). Results from intravenous dosing studies using 5 mg/kg in rats indicated a mean C0 of 74669.11 ng/mL, $t_{1/2}$(hours) of 3.86 hours, $AUC_{0\text{-last}}$ (ng·hour/mL) of 15,544.36, and $AUC_{0\text{-inf}}$ (ng·hour/mL) of 15,573.91. Results from oral dosing studies using 10 mg/kg in rats indicated a mean C_{max} (ng/mL) of 919.50, T_{max} (h) of 2.67, $AUC_{0\text{-last}}$ (ng·hour/mL) of 3,792.26, and $AUC_{0\text{-inf}}$ (ng·hour/mL) of 3,876.82. Ames test confirmed that EC359 did not induce an evident (significant) >2-fold increase in the revertant counts at the doses tested (dose related), in the tester strains both with and without metabolic activation according to the evaluation criteria mentioned in OECD guideline no.471. Hence, the compound EC359 is considered nonmutagenic with *Salmonella typhimurium* strains TA98, TA100, TA1535, TA1537, and *E.coli* combo, both with and without metabolic activation. In hERG cardiotoxicity screening, up to 30 μmol/L concentration of EC359 did not show 50% inhibition, hence no liability. Among CYP enzymes, EC359 inhibits 2D6, therefore, caution is warranted in concurrent administration of drugs that inhibits 2D6 such as Prozac. Metabolic stability and plasma stability are moderate in human with high plasma protein binding. Good bioavailability (pharmacokinetics) was observed in both intraperitoneal and oral dosing (Supplementary Fig. S9). Collectively, the data from these studies indicate EC359 has specific on-target activity (pharmacodynamics) and suggests EC359 as a druggable candidate for further development.

EC359 reduced the cell viability of LIF- and LIFR-expressing cells

We first examined the expression of LIF and LIFR in cells that represent various subtypes of TNBC (BT-549, SUM-159, MDA-MB-231, HCC1937, MDA-MB-468, and HCC1806), ER^+ breast cancer (MCF7 and T47D) as well as normal mammary epithelial cells (HMEC). We found that five of the six TNBC cells expressed high levels of LIF and LIFR when compared with ER^+ breast cancer cells and normal cells (Fig. 2A and B). Next, we examined the efficacy of EC359 on cell viability of TNBC and ER^+ breast cancer cells. Treatment with EC359 resulted in a significant dose-dependent reduction in the cell viability of TNBC cells (IC_{50} = 10–50 nmol/L) and their inhibition is well correlated with LIF and LIFR expression levels (Fig. 2C). Interestingly ER^+ breast cancer cells that express low levels of LIF and LIFR exhibited low sensitivity to EC359 treatment (IC_{50} > 1,000 nmol/L) when compared with TNBC cells (Fig. 2D). To further confirm the target specificity of EC359, we generated doxycycline-inducible LIFR-KO cells using Cas9 stably expressing TNBC cells. Results indicated a reduction of LIFR expression in BT-549 models contributed to the resistance of the EC359-mediated decrease in cell viability (Fig. 2E). Collectively, these data suggest that EC359 activity depends on presence of functional LIF/LIFR signaling axis in cells.

EC359 reduced survival and invasion and induced apoptosis of TNBC cells

We next examined the efficacy of the EC359 on the survival of TNBC cells. In clonogenic survival assays, EC359 significantly reduced the colony-forming ability of MDA-MB-231 and SUM-159 cells (Fig. 2F). Given the important role of the LIF axis in the invasiveness of cancer cells, we examined the effect of EC359 in reducing the invasion of TNBC cells. Matrigel invasion assays demonstrated that EC359 significantly reduced the invasion potential of MDA-MB-231 and BT-549 cells (Fig. 2G). Furthermore, we examined whether EC359 induced apoptosis in TNBC cells using caspase 3/7 activity assay and Annexin V staining assay. EC359 treatment significantly increased caspase-3/7 activity (Fig. 2H) and Annexin V–positive cells (Fig. 2I) in both MDA-MB-231 and BT-549 cells. Collectively, these results suggest that EC359 exhibits significant inhibitory activity on invasion and promotes apoptosis of TNBC cells.

EC359 inhibited LIFR-mediated transcriptional changes

LIF/LIFR activates multiple signaling pathways including JAK/STAT3, MAPK, AKT, and mTOR; all of which are implicated in TNBC progression. To confirm the inhibitory effect of EC359 on LIF/LIFR–mediated STAT3 activation, BT-549 cells that stably express STAT3-Luc reporter were pretreated with vehicle or EC359 followed by stimulation with LIF. As expected, LIF treatment significantly increased the STAT3 reporter activity and this activation was inhibited by EC359 treatment (Fig. 3A). Because our modeling studies predicted EC359 interaction with the ligand-binding interface of LIFR, we examined whether EC359 also blocks signaling by other LIFR ligands such as Oncostatin M

Published OnlineFirst May 29, 2019; DOI: 10.1158/1535-7163.MCT-18-1258

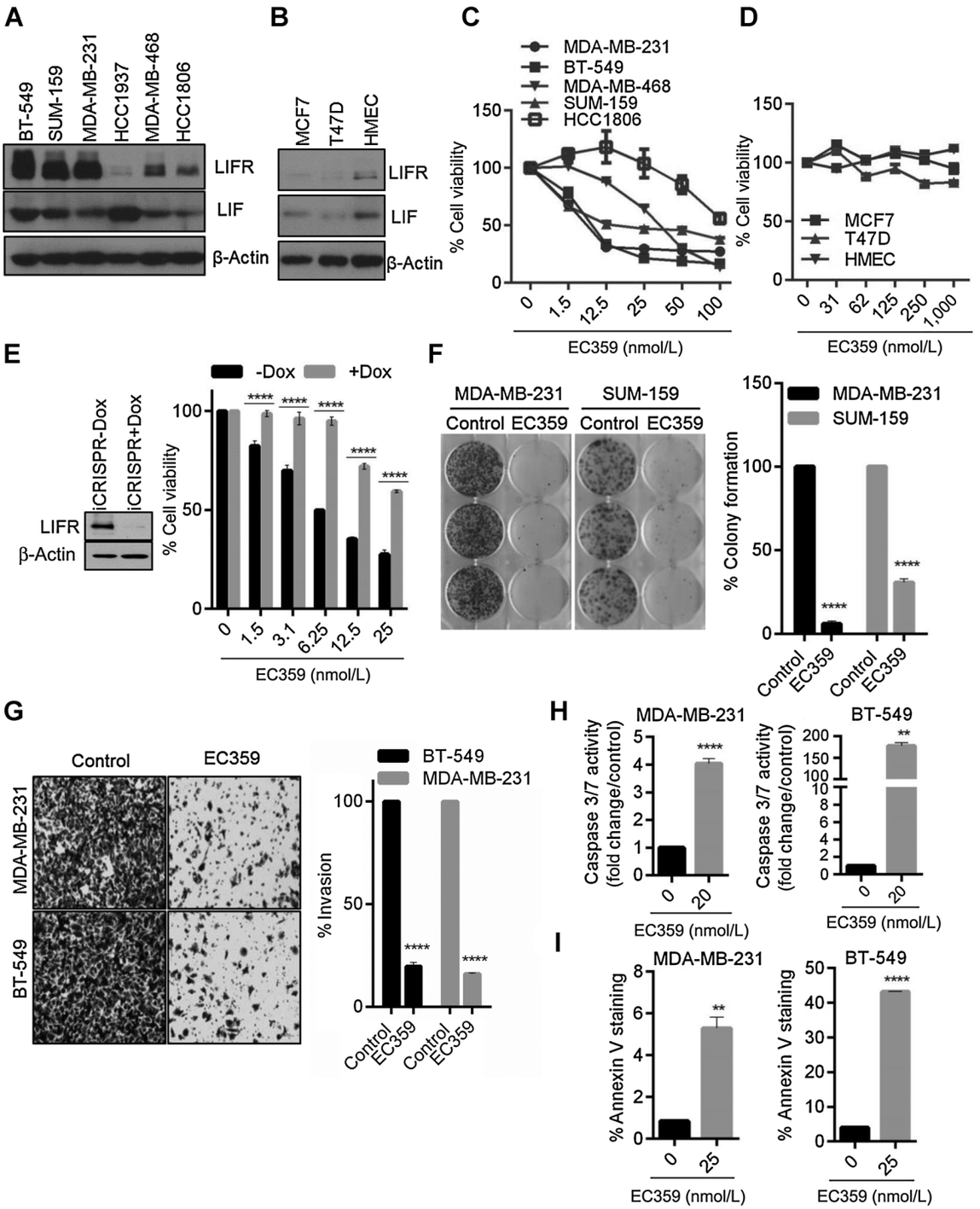

Figure 2.

EC359 decreases cell viability, colony formation, and invasion, and promotes apoptosis of TNBC cells that express LIF and LIFR. The expression of LIF and LIFR in TNBC (**A**), ER$^+$ breast cancer and normal mammary epithelial cells (**B**) was determined by Western blotting. Effect of increasing doses of EC359 on the cell viability of TNBC (**C**), ER$^+$ breast cancer and normal mammary epithelial cells (**D**) was determined using the MTT cell viability assay ($n = 3$). **E,** Effect of inducible CRISPR/Cas9-mediated KO of LIFR on EC359-induced cell viability was determined using MTT assays in BT-549 cells ($n = 3$). **F,** Effect of EC359 (20 nmol/L) on cell survival was measured using colony formation assays. **G,** Effect of EC359 (25 nmol/L) on cell invasion of MDA-MB-231 and BT-549 model cells was determined using Matrigel invasion chamber assays ($n = 3$). Representative images of invaded cells are shown, and the number of invaded cells in five random fields was quantitated. Effect of indicated doses of EC359 on caspase-3/7 activity (Caspase-Glo3/7 assay; **H**) and Annexin V staining in MDA-MB-231 and BT-549 cells ($n = 3$) was determined (**I**). **, $P < 0.01$; ****, $P < 0.0001$.

Published OnlineFirst May 29, 2019; DOI: 10.1158/1535-7163.MCT-18-1258

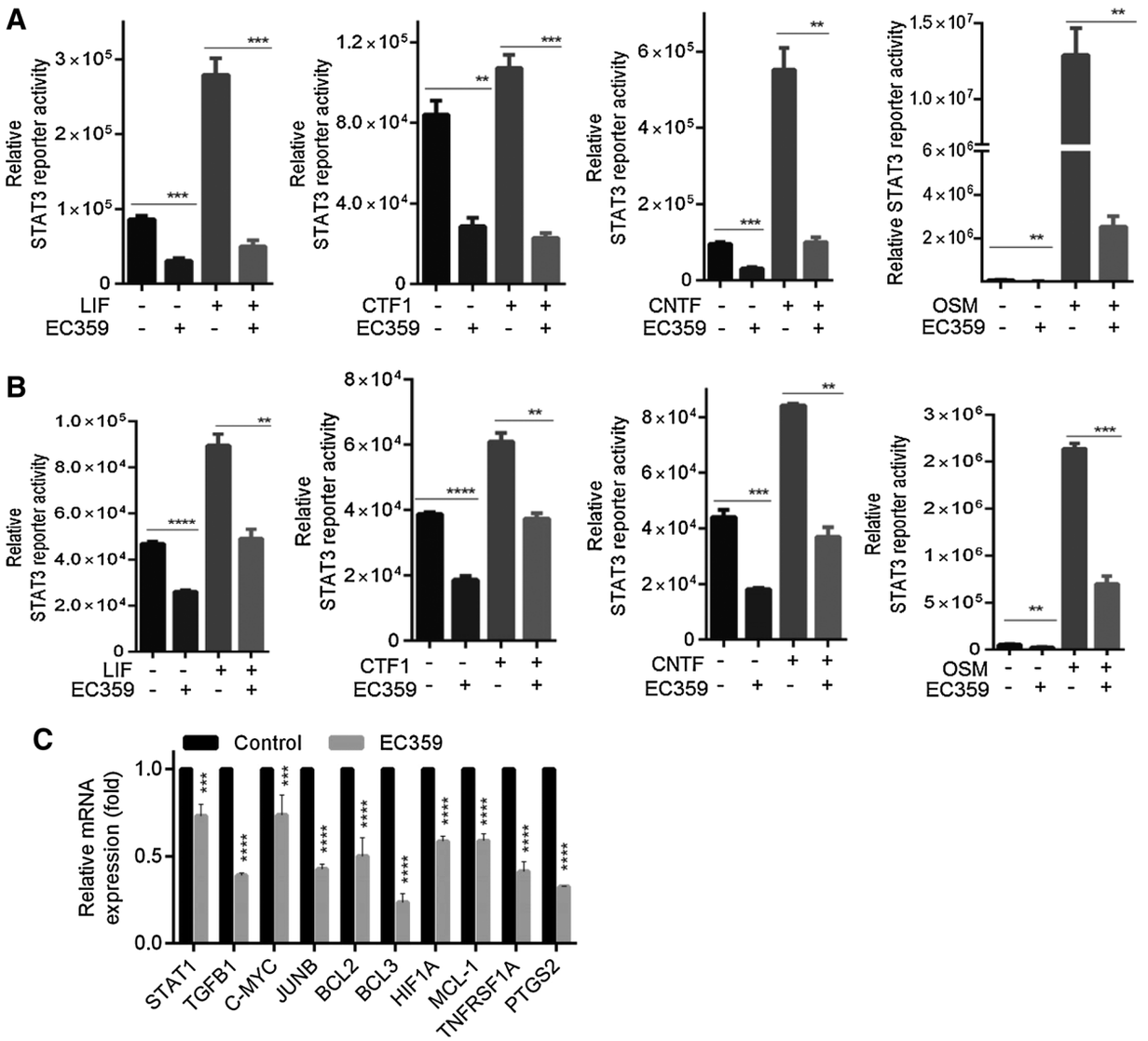

Figure 3.

Effect of EC359 on LIFR-mediated transcription in TNBC cells. BT-549 (**A**) and MDA-MB-231 (**B**) cells stably expressing STAT3-luc reporter were serum starved for 24 hours, pretreated with EC359 (50 nmol/L) for 1 hour, and then stimulated with LIF, CTF1, OSM, and CNTF ($n = 3$). Reporter activity was measured after 24 hours. **C,** Effect of EC359 (100 nmol/L) treatment (12 hours) on STAT3-targeted genes in BT549 cells was measured using qRT-PCR analysis ($n = 3$). **, $P < 0.01$; ***, $P < 0.001$; ****, $P < 0.0001$.

(OSM), Ciliary Neurotrophic Factor (CNTF), and Cardiotrophin 1 (CTF1). Results showed that EC359 blocked the OSM, CNTF, and CTF1-mediated STAT3 activity in BT-549 cells (Fig. 3A). We also confirmed that EC359 has the ability to block LIF-, OSM-, CNTF-, and CTF1-mediated STAT3 activation using MDA-MB-231 cells stably expressing STAT3-Luc reporter (Fig. 3B). In qRT-PCR assays using BT-549 cells, EC359 treatment significantly reduced the expression of several known STAT3 target genes (Fig. 3C).

EC359 reduced LIFR-mediated activation of downstream signaling pathways

To further confirm the effect of EC359 on LIF/LIFR downstream signaling pathways, MDA-MB-231 and BT-549 cells were pretreated with vehicle or EC359 and subsequently stimulated with LIF. STAT3 activation was examined using Western blotting. EC359 treatment substantially reduced the LIF activation of STAT3 in both BT-549 and MDA-MB-231 cells (Fig. 4A). EC359 also reduced the STAT3 activation by OSM and CNTF (Fig. 4B and C). In addition, EC359 treatment substantially decreased the phosphorylation of AKT, mTOR, S6, and ERK1/2 in MDA-MB-231 and BT-549 cells (Fig. 4D and E). EC359 treatment also increased the phosphorylation of proapoptotic p38MAPK in BT-549 cells (Fig. 4E). We confirmed whether alteration in downstream signaling seen upon EC359 treatment such as STAT3 occurs in the cell line that has a doxycycline-inducible deletion of the LIFR. Results showed that KO of LIFR significantly reduced the STAT3 activation (Supplementary Fig. S10A). Furthermore,

Published OnlineFirst May 29, 2019; DOI: 10.1158/1535-7163.MCT-18-1258

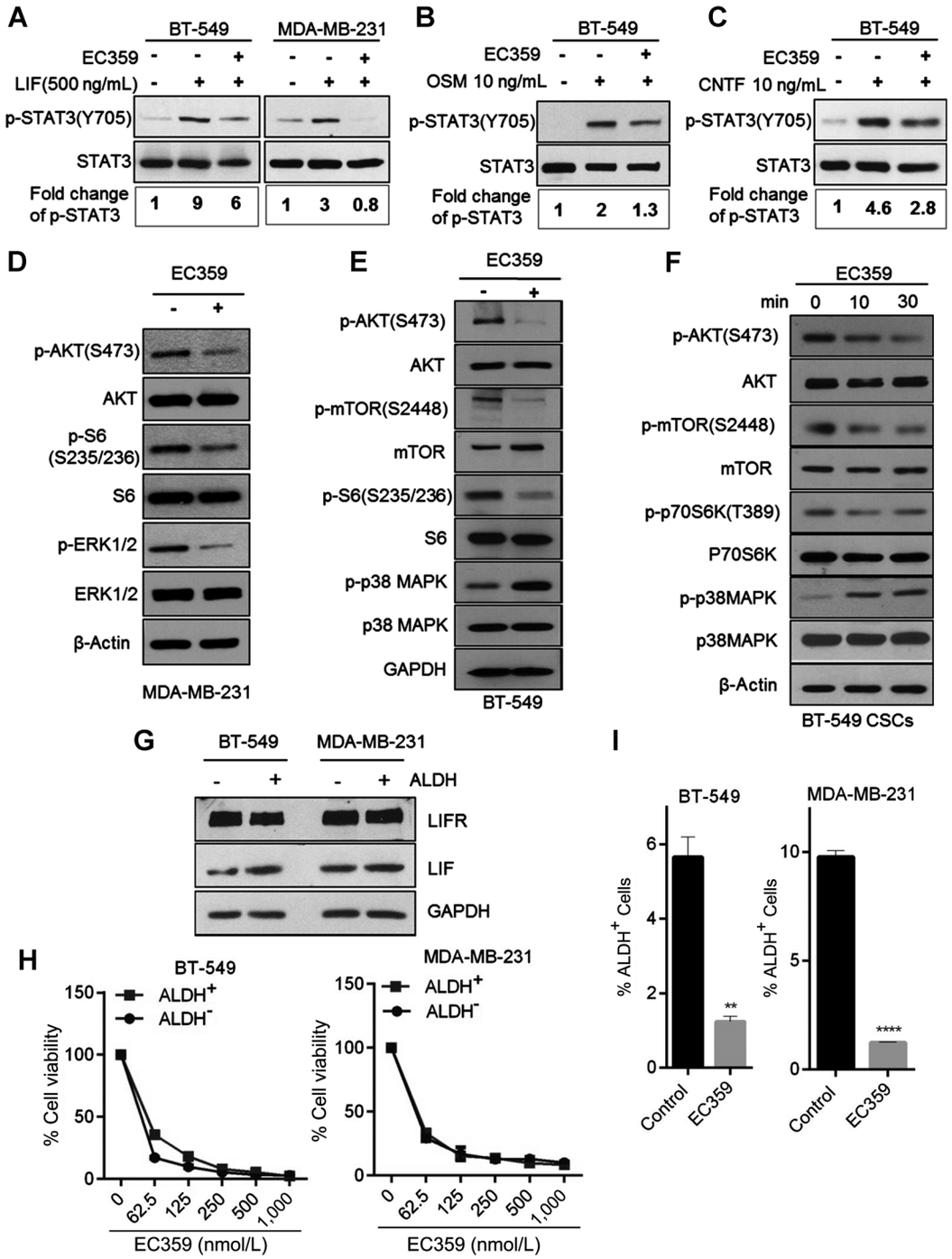

Figure 4.

EC359 inhibits LIFR downstream signaling and reduces stemness of TNBC cells. **A,** MDA-MB-231 and BT-549 cells were serum starved for 24 hours, pretreated with EC359 (100 nmol/L) for 1 hour, and then stimulated with LIF (10 minutes), and the status of STAT3 phosphorylation was measured using Western blotting. STAT3 phosphorylation was quantitated using ImageJ program, normalized to total STAT3, and shown as fold induction over control cells. BT-549 cells were serum starved for 24 hours, pretreated with EC359 (100 nmol/L) for 1 hour, and then stimulated with OSM (10 ng; **B**) and CNTF (10 ng; **C**) for 10 minutes, and the status of STAT3 phosphorylation was measured using Western blotting. **D–F,** MDA-MB-231, BT-549, and CSCs were treated with EC359 (100 nmol/L), and status of LIFR downstream signaling was measured using Western blotting. **G,** $ALDH^+$ and $ALDH^-$ cells were isolated by FACS, and the expression levels of LIFR and LIF were measured by Western blotting. **H,** Effect of EC359 on the viability of $ALDH^+$ (CSCs) and $ALDH^-$ (non-CSCs) cells was determined using CellTiter Glo assay ($n = 3$). **I,** BT-549 and MDA-MB-231 cells were treated with EC359 (100 nmol/L), and the status of $ALDH^+$ cells was determined by FACS analysis. **, $P < 0.01$; ****, $P < 0.0001$.

Published OnlineFirst May 29, 2019; DOI: 10.1158/1535-7163.MCT-18-1258

stimulation of LIFR KO cells with LIF did not activate STAT3 in this model. However, EC359 is able to block LIF-mediated STAT3 activation in LIFR-expressing control cells. These results confirm that the downstream effects seen in EC359 are due to its effects on LIFR and that STAT3 is a downstream effector of LIFR in TNBC cells (Supplementary Fig. S10A). These results suggest that EC359 acts as a LIFR inhibitor and attenuates LIF and other LIFR ligand–mediated signaling in TNBC cells.

EC359 reduced the cell viability and self-renewal of TNBC stem cells

The LIF/LIFR axis plays a vital role in stemness (6, 12). To test the effect of EC359 on stemness, CSCs were isolated from MDA-MB-231 and BT-549 using $ALDH^+$ flow cytometry sorting. EC359 treatment substantially decreased the phosphorylation of AKT, mTOR, p70S6K, and increased phosphorylation of proapoptotic p38MAPK in CSCs (Fig. 4F). Western blot analysis showed that $ALDH^+$ (CSCs) and $ALDH^-$ (non-CSCs) cells have similar levels of LIFR (Fig. 4G). Furthermore, in cell viability assays, EC359 similarly inhibited both $ALDH^+$ and $ALDH^-$ cells (Fig. 4H). To further study the effect of EC359 on the self-renewal ability of CSCs, extreme limiting dilution assays (ELDA) were performed. Results showed that EC359 significantly reduced the self-renewal of CSCs compared with control (Supplementary Fig. S10B). Furthermore, pretreatment of TNBC cells with EC359 significantly reduced the abundance of $ALDH^+$ cells (Fig. 4I).

EC359 reduced TNBC xenograft tumor growth *in vivo*

To test the efficacy of EC359 on *in vivo* tumor progression, we established MDA-MB-231 xenograft tumors in the mammary fat pad of nude mice. Mice were randomized to vehicle (hydroxymethylcellulose) and EC359 (5 mg/kg/day via subcutaneous injection) 3 days/week. EC359 treatment significantly reduced the tumor progression compared with vehicle (Fig. 5A). The body weights of mice in the vehicle and EC359-treated groups remained unchanged (Fig. 5B) confirming the low toxicity of EC359. Moreover, EC359-treated tumors exhibited fewer proliferating cells (Ki-67–positive cells) compared with vehicle-treated tumors (Fig. 5C). In addition, qRT-PCR analysis confirmed significant decrease in the activation of STAT3 target genes in EC359-treated tumors compared with vehicle (Fig. 5D). Western blot analysis confirmed that xenograft tumors express LIFR and LIF (Fig. 5E). Furthermore, EC359 treatment substantially reduced the phosphorylation of STAT3, ERK1/2, and AKT in tumors compared with vehicle-treated tumors (Fig. 5E). Collectively, these results suggest that EC359 has potent antitumor activity on TNBC in preclinical models.

EC359 has activity against primary patient-derived TNBC explants and reduced *in vivo* tumor progression in PDX model

We tested the utility of EC359 using an *ex vivo* culture model of primary breast tumors, which allowed for the evaluation of drugs on human tumors while maintaining their native tissue architecture (Fig. 6A). Briefly, surgically extirpated deidentified TNBC tissues were cut into small pieces and placed on gelatin sponge soaked in the culture medium and grown for a short term in the presence of vehicle or EC359 (Fig. 6A). Treatment of TNBC explants with EC359 substantially decreased their proliferation (Ki-67 positivity) compared with vehicle-treated tumors (Fig. 6B and C). Next, we tested the effect of EC359 on PDX tumor growth *in vivo*. EC359 treatment significantly reduced the tumor progression compared with the vehicle-treated control group (Fig. 6D) and did not affect the body weight (Fig. 6E). EC359-treated PDX tumors exhibited fewer proliferating cells compared with vehicle-treated tumors (Fig. 6F). qRT-PCR analysis confirmed a significant decrease in the activation of STAT3 target genes in EC359-treated mice (Fig. 6G). Western blot analysis confirmed that PDX tumors express LIFR and LIF (Fig. 6H). Furthermore, EC359 treatment substantially reduced the phosphorylation of mTOR, S6, and AKT in tumors compared with vehicle-treated tumors (Fig. 6H). These results suggest that EC359 has therapeutic activity in primary patient-derived TNBC explants and PDX tumors.

Discussion

LIF is the most pleiotropic member of the IL6 family of cytokines (4) that signals via the LIFR (5). Recent evidence suggested tumors exhibit upregulated LIF/LIFR signaling via autocrine and paracrine mechanisms (1, 5–7). However, lack of specific inhibitors targeting the LIF/LIFR axis represents a critical barrier in the field. In this study, we rationally designed a small organic molecule, EC359 that emulates the LIF/LIFR-binding site and functions as a first-in-class LIFR inhibitor from a library of compounds. Using multiple TNBC cells, we demonstrated that EC359 decreases cell viability, invasion, and promotes apoptosis. Mechanistic studies using Western blot, reporter gene assays, and qRT-PCR confirmed significant reduction of activation of LIF/LIFR-mediated pathways. Utilizing PDX, and patient-derived explant (PDEx) models, we demonstrated the *in vivo* efficacy of EC359.

The molecular modeling and SPR suggests the putative binding site is at the interface of LIF and LIFR. EC359 may display longer resident time (i.e., slower k_{off}) in the LIF/LIFR complex as suggested by the molecular model. Reasonable (about 30 minutes) residence time ($1/k_{off}$) suggests it may display biological activity *in vitro* and *in vivo*. However, potency of EC359 may depend on the concentration of LIF. During the SPR assay, we noted that EC359 was incompletely dissolved in the running buffer. Thus, due to poor solubility of the inhibitor in running buffer (inhibitor precipitates at concentrations 25–50 μmol/L in 5% DMSO) derived kinetic constants must be considered approximate; spiking at 2 μmol/L (green color) suggest that the compound may be aggregated; microaggregation affects not only the transport property of the ligands, but also the off-rate. Thus, the weaker binding affinity derived from SPR studies is likely due to poor solubility of the compound, which may be attributed as limitation of SPR technique. Nonetheless, results from SPR show that EC359 is specific to LIFR.

Recently, the MST technique has been widely used for characterizing protein–ligand interactions. MST offers a unique advantage over conventional isothermal titration calorimetry (ITC); unlike SPR, in MST, the target is not immobilized, and ligand-binding is independent of size or physical properties of ligands. MST analysis indicated higher binding affinity (K_d) between LIF and LIFR (1.36 nmol/L) than LIFR and EC359 (10.2 nmol/L). Also, the longer residence time/slower k_{off} in SPR demonstrates this pertinent biological effect. These values were consistent with high nanomolar potency of EC359 *in vitro* and *in vivo*. The discrepancy in the binding affinity measured between SPR and MST assays may be due to either difference in steady-state binding (MST) versus kinetic binding (SPR), or drug-induced structural changes upon binding; structural changes at the binding site, or

Published OnlineFirst May 29, 2019; DOI: 10.1158/1535-7163.MCT-18-1258

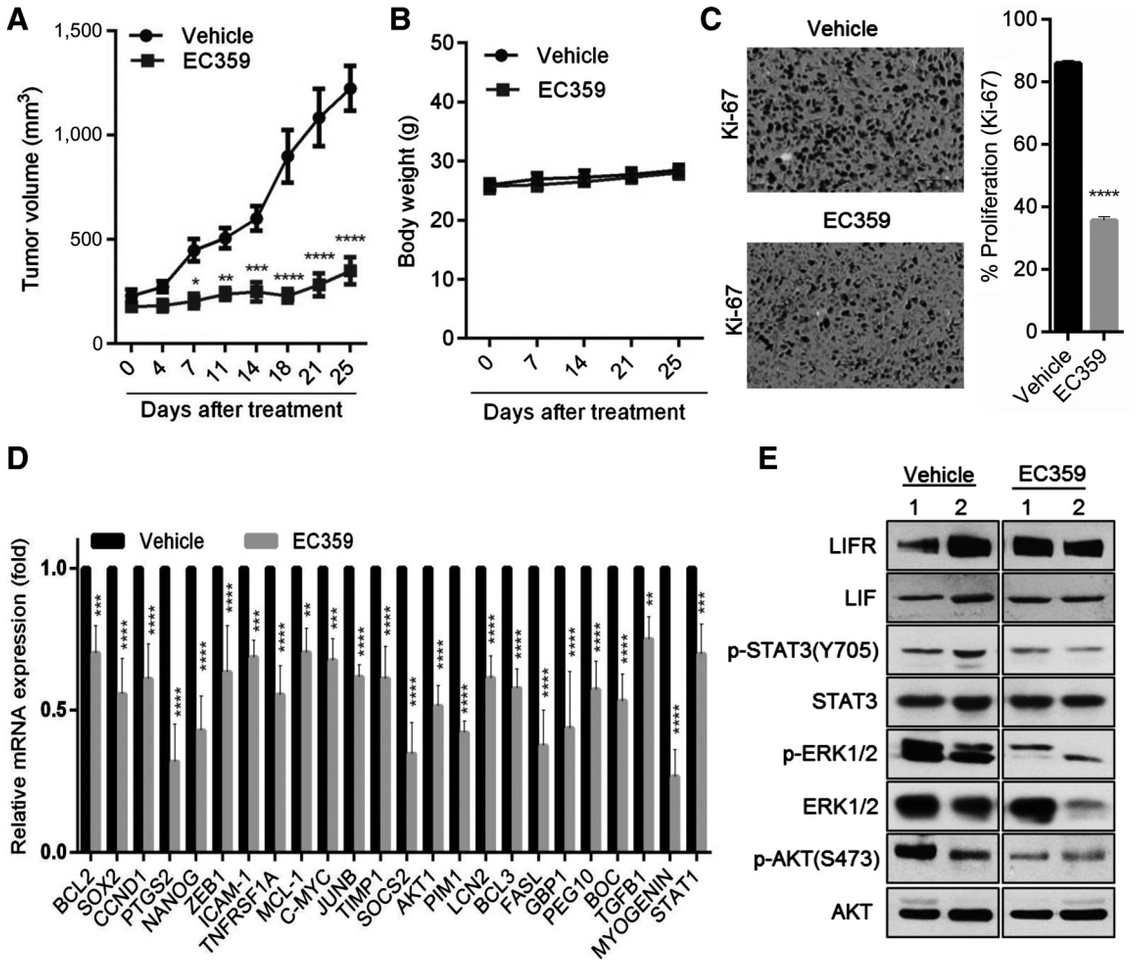

Figure 5.

EC359 inhibits the growth of TNBC xenograft tumors. **A,** MDA-MB-231 xenografts ($n = 8$) were treated with vehicle or EC359 (5mg/kg/s.c./3 days/week). Tumor volumes are shown. **B,** Body weights of vehicle and EC359-treated mice are shown. **C,** Ki-67 expression as a marker of proliferation was analyzed by IHC and quantitated. **D,** Status of STAT3 target genes was measured using qRT-PCR analysis ($n = 3$). **E,** LIFR downstream signaling was measured using Western blotting (data using two different xenograft tumors are shown). *, $P < 0.05$; **, $P < 0.01$; ***, $P < 0.001$; ****, $P < 0.0001$.

both. Despite the differences in SPR and MST techniques, our results show that EC359 directly binds and disrupts the LIFR signaling complex.

The LIF/LIFR axis exhibits differential effects, which depended on the cell type, including stimulating or inhibiting cell proliferation, differentiation, and survival (4, 11, 24). LIFR is also reported to function as a metastasis suppressor through the Hippo–YAP pathway (35) and confer a dormancy phenotype in breast cancer cells disseminating to bone (36). It should be noted that presence of LIF is important for LIFR activation as we have determined in our SPR analysis. Hence studies using low LIF-expressing cell lines such as MCF-7 or T47D may not have an overly active LIF/LIFR signaling. However, LIFR signaling is complex as multiple ligands activate LIFR including LIF, CNTF, OSM, and CTF1. Despite the ability of LIF to activate JAK1/STAT3, PI3K/AKT, and MAPK pathways in these cell lines, differences in signaling outcome may, in part, arise from differential levels of activation of these three pathways, multiple ligands to LIFR, and differences in tumor microenvironment (TME; refs. 1, 37).

Earlier studies revealed that LIF, CTF1, and OSM share an overlapping binding site located in the Ig-like domain of LIFR and different behaviors of LIF, CTF1, and OSM can be related to the different affinity of their site for LIFR (38). Our modeling studies predicted that EC359 will interact at the LIF–LIFR binding interface and block interaction of LIF to LIFR. In agreement with published studies, our reporter assays and Western blot analyses showed that EC359 has the ability to block the signaling mediated by other cytokines (CTF1, CNTF, and OSM) that interact LIFR at LIF/LIFR interface. Blockage of LIFR by EC359 can leverage additional benefit of interfering the LIFR–JAK–STAT pathway by all known four LIFR ligands. We speculate that the unique ability of EC359 to bind the common ligand-binding site blocks multiple ligands' interactions with LIFR offers an advantage over other biologics or small molecules that can only target either of these ligands alone. This may also account the apparent differences in the activity seen by EC359 in TNBC and ER^+ breast cancer as TNBC expresses higher levels LIFR ligands compared with ER^+

Published OnlineFirst May 29, 2019; DOI: 10.1158/1535-7163.MCT-18-1258

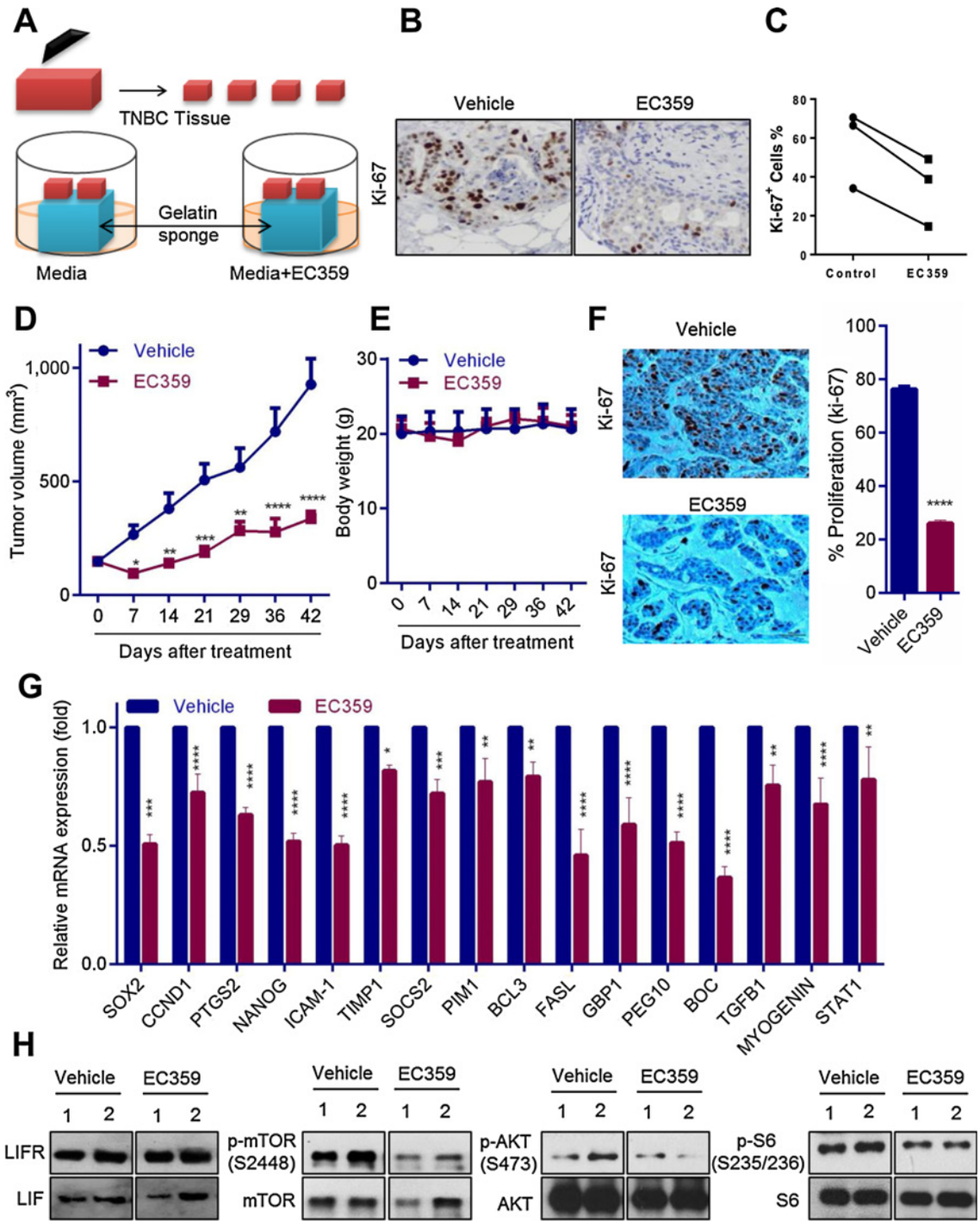

Figure 6.

EC359 decreases the growth of primary patient-derived TNBC explants *ex vivo* and PDX tumors *in vivo.* **A,** Schematic representation of *ex vivo* culture model. **B,** TNBC explants were treated with EC359 for 72 hours, and the proliferation was determined using Ki-67 immunostaining. Representative Ki-67 staining from one tumor treated with vehicle or EC359 is shown. **C,** The Ki67 expression in TNBC explants ($n = 3$) is quantitated. **D,** TNBC PDX tumors ($n = 6$) were treated with vehicle or EC359 (10 mg/kg/s.c./3 days/week). Tumor volumes are shown. **E,** Body weights of vehicle and EC359-treated mice are shown. **F,** Ki-67 expression as a marker of proliferation was analyzed by IHC and quantitated. **G**, STAT3 target genes were measured by using qRT-PCR analysis ($n = 3$). **H,** Status of LIFR downstream signaling was measured using Western blotting (data using two different PDX tumors are shown). *, $P < 0.05$; **, $P < 0.01$; ***, $P < 0.001$; ****, $P < 0.0001$.

Published OnlineFirst May 29, 2019; DOI: 10.1158/1535-7163.MCT-18-1258

breast cancer. In SPR studies, we found that the presence of ligand LIF further enhanced LIFR interaction with EC359 compared with LIFR alone. Because the ER^+ breast cancer cells lack or possess low levels of LIF and LIFR, the increased fold difference in activity (sensitivity) of EC359 toward TNBC cells may reflect presence of increased ligand/receptor levels in TNBC. Furthermore, EC359 is unable to block OSM, CTF1, and CNTF, interactions with their natural receptors (OSMR/gp130, LST/gp130, CNTFR/gp130 respectively); therefore, EC359 is less likely to affect the physiologic signaling of CTF1, CNTF, and OSM. As a consequence, the issue of toxicity is less likely to occur. Accordingly, in xenograft studies, we did not observe toxicity over the course of EC359 treatment. However, future studies using formal toxicity protocols are needed to address the toxicity concerns and is beyond the current scope of this work.

Breast cancer cells often exhibit autocrine stimulation of LIF–LIFR axis. Some subtypes of TNBC such as claudin-low are highly enriched for CSC markers (39, 40). The LIF promoter is hypermethylated in normal breast epithelial cells, but extensively demethylated during breast cancer progression (5). TNBC cells have higher expression of LIF and LIFR compared with ER^+ breast cancer cells and overexpression of LIF is significantly associated with a poorer relapse-free survival in patients with breast cancer (4). Together, these emerging findings strongly suggest that LIF signaling in TNBC may be clinically actionable and that disruption of the LIF signaling cascade has potential to block progression of subtypes of TNBC that exhibit a LIF/LIFR autocrine loop.

LIF activates multiple signaling pathways via LIFR including STAT3, MAPK, AKT, and mTOR (3, 4)—all are implicated in cancer progression. Tumors exhibit upregulated LIF–JAK–STAT3 signaling via autocrine and paracrine mechanisms (1, 5–7). LIF signaling also plays a role in crosstalk between tumor cells and fibroblasts, and mediates the proinvasive activation of stromal fibroblasts (9). LIF/LIFR signaling is implicated in modulation of multiple immune cell types present in tumor microenvironment (TME) including T-eff, T-reg, macrophages (41), and myeloid cells, which results in immune suppression (42). In our studies using TNBC model cells, we found that EC359 substantially reduced the activation of STAT3, MAPK, AKT, and mTOR; and significantly delayed tumor progression *in vivo*. However, our mechanistic studies are limited to EC359 effects on epithelial cells; future studies are needed to clearly examine the effect of EC359 on TME.

LIF and LIFR are overexpressed in multiple solid tumors (5, 7, 43). While LIF can act on a wide range of cell types, LIF knockout mice have revealed that many of these actions are not apparent during ordinary development (1), indicating a potential therapeutic window for LIF/LIFR axis inhibitors in addition to less toxicity in normal adult tissues. Considering the importance of the LIF/LIFR axis in cancer, humanized anti LIF antibody (MSC-1) that blocks LIF signaling is being tested in a phase I clinical trial mode to determine its safety and tolerability (ClinicalTrials.gov, NCT03490669). Given the wide deregulation of the LIF/LIFR axis in multiple tumors, the small-molecule LIFR inhibitor EC359 may have utility in treating other solid tumors including glioblastoma, ovarian cancer, colon cancer, and pancreatic cancer all of which exhibit dysregulated LIF/LIFR signaling. Our studies only examined the utility of EC359 using TNBC models. Future studies are needed to further evaluate the effects of EC359 in other cancer models and to examine any potential beneficial effects of EC359 on TME.

In summary, our data demonstrated that EC359 is a highly potent and specific LIFR inhibitor. EC359 blocked LIF/LIFR physical and functional interaction, signaling, and reduced cell viability of LIF/LIFR–expressing TNBC cells both *in vitro* and *in vivo*. EC359 represents a exciting new mechanism to modulate LIF/LIFR oncogenic functions. Because EC359 is a small, stable molecule, it is amenable for translation to clinical trials for patients with TNBC as either monotherapy or in combination with current standard of care.

Disclosure of Potential Conflicts of Interest

G.V. Raj is a founder at EtiraRx and GaudiumRx, reports receiving a commercial research grant from Bayer, has received speakers' bureau honoraria from Bayer, Janssen, Astellas, and Pfizer, is a consultant/advisory board member for Bayer and Janssen. K.J. Nickisch has ownership interest (including stock, patents, etc.) from Evestra. No potential conflicts of interest were disclosed by the other authors.

Authors' Contributions

Conception and design: S. Viswanadhapalli, G.R. Sareddy, B. Santhamma, A. Chávez-Riveros, G.V. Raj, A.J. Brenner, R.R. Tekmal, H.B. Nair, K.J. Nickisch, R.K. Vadlamudi

Development of methodology: S. Viswanadhapalli, G.R. Sareddy, B. Santhamma, A. Chávez-Riveros, M. Bajda, A.J. Brenner

Acquisition of data (provided animals, acquired and managed patients, provided facilities, etc.): S. Viswanadhapalli, Y. Luo, M. Zhou, M. Li, S. Ma, R. Sonavane, U.P. Pratap, X. Li, A. Chang, A. Chávez-Riveros, X. Pan, R. Murali, M. Bajda, G.V. Raj, M.K. Rao, R.R. Tekmal

Analysis and interpretation of data (e.g., statistical analysis, biostatistics, computational analysis): S. Viswanadhapalli, Y. Luo, G.R. Sareddy, M. Li, R. Sonavane, U.P. Pratap, A. Chang, A. Chávez-Riveros, K.V. Dileep, K.Y.J. Zhang, X. Pan, M. Bajda, R.K. Vadlamudi

Writing, review, and/or revision of the manuscript: S. Viswanadhapalli, G.R. Sareddy, B. Santhamma, K.A. Altwegg, K.V. Dileep, K.Y.J. Zhang, R. Murali, M. Bajda, G.V. Raj, A.J. Brenner, M.K. Rao, H.B. Nair, K.J. Nickisch, R.K. Vadlamudi

Administrative, technical, or material support (i.e., reporting or organizing data, constructing databases): G.V. Raj, V. Manthati

Study supervision: R.K. Vadlamudi

Other (conducted modeling studies): K.V. Dileep, K.Y.J. Zhang

Acknowledgments

We thank Jessica Perry (Ob/Gyn UT Health San Antonio) for proofreading of the manuscript. MST studies were performed by 2bind GmbH, Germany. K.V. Dileep thanks Japan Society for the Promotion of Science for a postdoctoral fellowship. This study was supported by the DOD BCRP grant W81XWH-18-1-0016 (to R.K. Vadlamudi and K.J. Nickisch), DOD BCRP grant W81XWH-16-0294 (to R.R. Tekmal), NCI Cancer Center Support Grant P30CA054174-17, Max and Minnie Tomerlin Voelcker Fund (to G.R. Sareddy), and NIH grant 1R01CA179120-01 (to R.K. Vadlamudi and M. Rao).

The costs of publication of this article were defrayed in part by the payment of page charges. This article must therefore be hereby marked *advertisement* in accordance with 18 U.S.C. Section 1734 solely to indicate this fact.

Received November 6, 2018; revised March 12, 2019; accepted May 16, 2019; published first May 29, 2019.

References

1. Nicola NA, Babon JJ. Leukemia inhibitory factor (LIF). Cytokine Growth Factor Rev 2015;26:533–44.
2. Stahl N, Boulton TG, Farruggella T, Ip NY, Davis S, Witthuhn BA, et al. Association and activation of Jak-Tyk kinases by CNTF-LIF-OSM-IL-6 beta receptor components. Science 1994;263:92–5.
3. Liu SC, Tsang NM, Chiang WC, Chang KP, Hsueh C, Liang Y, et al. Leukemia inhibitory factor promotes nasopharyngeal carcinoma progression and radioresistance. J Clin Invest 2013;123:5269–83.
4. Li X, Yang Q, Yu H, Wu L, Zhao Y, Zhang C, et al. LIF promotes tumorigenesis and metastasis of breast cancer through the AKT-mTOR pathway. Oncotarget 2014;5:788–801.
5. Shin JE, Park SH, Jang YK. Epigenetic up-regulation of leukemia inhibitory factor (LIF) gene during the progression to breast cancer. Mol Cells 2011; 31:181–9.
6. Penuelas S, Anido J, Prieto-Sanchez RM, Folch G, Barba I, Cuartas I, et al. TGF-beta increases glioma-initiating cell self-renewal through the induction of LIF in human glioblastoma. Cancer Cell 2009;15:315–27.
7. Wu L, Yu H, Zhao Y, Zhang C, Wang J, Yue X, et al. HIF-2alpha mediates hypoxia-induced LIF expression in human colorectal cancer cells. Oncotarget 2015;6:4406–17.
8. Guo H, Cheng Y, Martinka M, McElwee K. High LIFr expression stimulates melanoma cell migration and is associated with unfavorable prognosis in melanoma. Oncotarget 2015;6:25484–98.
9. Albrengues J, Bourget I, Pons C, Butet V, Hofman P, Tartare-Deckert S, et al. LIF mediates proinvasive activation of stromal fibroblasts in cancer. Cell Rep 2014;7:1664–78.
10. Morton SD, Cadamuro M, Brivio S, Vismara M, Stecca T, Massani M, et al. Leukemia inhibitory factor protects cholangiocarcinoma cells from drug-induced apoptosis via a PI3K/AKT-dependent Mcl-1 activation. Oncotarget 2015;6:26052–64.
11. Kellokumpu-Lehtinen P, Talpaz M, Harris D, Van Q, Kurzrock R, Estrov Z. Leukemia-inhibitory factor stimulates breast, kidney and prostate cancer cell proliferation by paracrine and autocrine pathways. Int J Cancer 1996; 66:515–9.
12. Cartwright P, McLean C, Sheppard A, Rivett D, Jones K, Dalton S. LIF/STAT3 controls ES cell self-renewal and pluripotency by a Myc-dependent mechanism. Development 2005;132:885–96.
13. Kuphal S, Wallner S, Bosserhoff AK. Impact of LIF (leukemia inhibitory factor) expression in malignant melanoma. Exp Mol Pathol 2013;95: 156–65.
14. Liu J, Yu H, Hu W. LIF is a new p53 negative regulator. J Nat Sci 2015;1: e131.
15. Liu B, Lu Y, Li J, Liu Y, Liu J, Wang W. Leukemia inhibitory factor promotes tumor growth and metastasis in human osteosarcoma via activating STAT3. APMIS 2015;123:837–46.
16. Kamohara H, Ogawa M, Ishiko T, Sakamoto K, Baba H. Leukemia inhibitory factor functions as a growth factor in pancreas carcinoma cells: involvement of regulation of LIF and its receptor expression. Int J Oncol 2007;30:977–83.
17. Shin JE, Park SH, Jang YK. Epigenetic up-regulation of leukemia inhibitory factor (LIF) gene during the progression to breast cancer. Mol Cells 2011; 31:181–9.
18. Foulkes WD, Smith IE, Reis-Filho JS. Triple-negative breast cancer. N Engl J Med 2010;363:1938–48.
19. Carey L, Winer E, Viale G, Cameron D, Gianni L. Triple-negative breast cancer: disease entity or title of convenience? Nat Rev Clin Oncol 2010;7: 683–92.
20. Comprehensive molecular portraits of human breast tumours. Nature 2012;490:61–70.
21. Li Y, Zhang H, Zhao Y, Wang C, Cheng Z, Tang L, et al. A mandatory role of nuclear PAK4-LIFR axis in breast-to-bone metastasis of ERalpha-positive breast cancer cells. Oncogene 2019;38:808–21.
22. Quaglino A, Schere-Levy C, Romorini L, Meiss RP, Kordon EC. Mouse mammary tumors display Stat3 activation dependent on leukemia inhibitory factor signaling. Breast Cancer Res 2007;9:R69.
23. Dhingra K, Sahin A, Emami K, Hortobagyi GN, Estrov Z. Expression of leukemia inhibitory factor and its receptor in breast cancer: a potential autocrine and paracrine growth regulatory mechanism. Breast Cancer Res Treat 1998;48:165–74.
24. Yue X, Zhao Y, Zhang C, Li J, Liu Z, Liu J, et al. Leukemia inhibitory factor promotes EMT through STAT3-dependent miR-21 induction. Oncotarget 2016;7:3777–90.
25. Raj GV, Sareddy GR, Ma S, Lee TK, Viswanadhapalli S, Li R, et al. Estrogen receptor coregulator binding modulators (ERXs) effectively target estrogen receptor positive human breast cancers. Elife 2017;6. doi: 10.7554/eLife.26857.
26. Sareddy GR, Viswanadhapalli S, Surapaneni P, Suzuki T, Brenner A, Vadlamudi RK. Novel KDM1A inhibitors induce differentiation and apoptosis of glioma stem cells via unfolded protein response pathway. Oncogene 2017;36:2423–34.
27. Skiniotis G, Lupardus PJ, Martick M, Walz T, Garcia KC. Structural organization of a full-length gp130/LIF-R cytokine receptor transmembrane complex. Mol Cell 2008;31:737–48.
28. Huyton T, Zhang JG, Luo CS, Lou MZ, Hilton DJ, Nicola NA, et al. An unusual cytokine:Ig-domain interaction revealed in the crystal structure of leukemia inhibitory factor (LIF) in complex with the LIF receptor. Proc Natl Acad Sci U S A 2007;104:12737–42.
29. Halgren T. New method for fast and accurate binding-site identification and analysis. Chem Biol Drug Des 2007;69:146–8.
30. Genheden S, Ryde U. The MM/PBSA and MM/GBSA methods to estimate ligand-binding affinities. Expert Opin Drug Discov 2015;10:449–61.
31. Roy SS, Gonugunta VK, Bandyopadhyay A, Rao MK, Goodall GJ, Sun LZ, et al. Significance of PELP1/HDAC2/miR-200 regulatory network in EMT and metastasis of breast cancer. Oncogene 2014;33:3707–16.
32. Robinson RC, Grey LM, Staunton D, Vankelecom H, Vernallis AB, Moreau JF, et al. The crystal structure and biological function of leukemia inhibitory factor: implications for receptor binding. Cell 1994;77:1101–16.
33. Seidel SA, Dijkman PM, Lea WA, van den Bogaart G, Jerabek-Willemsen M, Lazic A, et al. Microscale thermophoresis quantifies biomolecular interactions under previously challenging conditions. Methods 2013;59:301–15.
34. Jerabek-Willemsen M, Wienken CJ, Braun D, Baaske P, Duhr S. Molecular interaction studies using microscale thermophoresis. Assay Drug Dev Technol 2011;9:342–53.
35. Chen D, Sun Y, Wei Y, Zhang P, Rezaeian AH, Teruya-Feldstein J, et al. LIFR is a breast cancer metastasis suppressor upstream of the Hippo-YAP pathway and a prognostic marker. Nat Med 2012;18:1511–7.
36. Johnson RW, Finger EC, Olcina MM, Vilalta M, Aguilera T, Miao Y, et al. Induction of LIFR confers a dormancy phenotype in breast cancer cells disseminated to the bone marrow. Nat Cell Biol 2016;18: 1078–89.
37. Auernhammer CJ, Melmed S. Leukemia-inhibitory factor-neuroimmune modulator of endocrine function. Endocr Rev 2000;21:313–45.
38. Plun-Favreau H, Perret D, Diveu C, Froger J, Chevalier S, Lelievre E, et al. Leukemia inhibitory factor (LIF), cardiotrophin-1, and oncostatin M share structural binding determinants in the immunoglobulin-like domain of LIF receptor. J Biol Chem 2003;278:27169–79.
39. D'Amato NC, Ostrander JH, Bowie ML, Sistrunk C, Borowsky A, Cardiff RD, et al. Evidence for phenotypic plasticity in aggressive triple-negative breast cancer: human biology is recapitulated by a novel model system. PLoS One 2012;7:e45684.
40. Perou CM. Molecular stratification of triple-negative breast cancers. Oncologist 2010;15:39–48.
41. Duluc D, Delneste Y, Tan F, Moles MP, Grimaud L, Lenoir J, et al. Tumor-associated leukemia inhibitory factor and IL-6 skew monocyte differentiation into tumor-associated macrophage-like cells. Blood 2007;110: 4319–30.
42. Zhao X, Ye F, Chen L, Lu W, Xie X. Human epithelial ovarian carcinoma cell-derived cytokines cooperatively induce activated CD4+CD25-CD45RA+ naive T cells to express forkhead box protein 3 and exhibit suppressive ability in vitro. Cancer Sci 2009;100:2143–51.
43. Bressy C, Lac S, Nigri J, Leca J, Roques J, Lavaut MN, et al. LIF drives neural remodeling in pancreatic cancer and offers a new candidate biomarker. Cancer Res 2018;78:909–21.

AACR American Association for Cancer Research

Molecular Cancer Therapeutics

EC359: A First-in-Class Small-Molecule Inhibitor for Targeting Oncogenic LIFR Signaling in Triple-Negative Breast Cancer

Suryavathi Viswanadhapalli, Yiliao Luo, Gangadhara R. Sareddy, et al.

Mol Cancer Ther 2019;18:1341-1354. Published OnlineFirst May 29, 2019.